

AD A117575

ARL F300057

AD

MEMORANDUM REPORT ARBRL-MR-03185  
(Supersedes IMR No. 695)

YAWSONDE TESTS FOR PROTOTYPES OF THE  
155MM INTERMEDIATE VOLATILITY  
AGENT PROJECTILE

William P. D'Amico, Jr.  
Wallace H. Clay

July 1982



US ARMY ARMAMENT RESEARCH AND DEVELOPMENT COMMAND  
BALLISTIC RESEARCH LABORATORY  
ABERDEEN PROVING GROUND, MARYLAND

Approved for public release; distribution unlimited.

DTIC FILE COPY

DTIC  
ELECTE  
JUL 29 1982  
S D  
D

82 07 06 084

Destroy this report when it is no longer needed.  
Do not return it to the originator.

Secondary distribution of this report by originating  
or sponsoring activity is prohibited.

Additional copies of this report may be obtained  
from the National Technical Information Service,  
U.S. Department of Commerce, Springfield, Virginia  
22161.

The findings in this report are not to be construed as  
an official Department of the Army position, unless  
so designated by other authorized documents.

*The use of trade names or manufacturers' names in this report  
does not constitute endorsement of any commercial product.*

UNCLASSIFIED

SECURITY CLASSIFICATION OF THIS PAGE (When Data Entered)

REPORT DOCUMENTATION PAGE		READ INSTRUCTIONS BEFORE COMPLETING FORM
1. REPORT NUMBER Memorandum Report ARBRL-MR-03185	2. GOVT ACCESSION NO. AD-A117 575	3. RECIPIENT'S CATALOG NUMBER
4. TITLE (and Subtitle) Yawsonde Tests for Prototypes of the 155mm Intermediate volatility Agent Projectile		5. TYPE OF REPORT & PERIOD COVERED Final
		6. PERFORMING ORG. REPORT NUMBER
7. AUTHOR(s) William P. D'Amico, Jr. Wallace H. Clay		8. CONTRACT OR GRANT NUMBER(s)
9. PERFORMING ORGANIZATION NAME AND ADDRESS US Army Ballistic Research Laboratory ATTN: DRDAR-BLL Aberdeen Proving Ground, MD 21005		10. PROGRAM ELEMENT, PROJECT, TASK AREA & WORK UNIT NUMBERS RDT&E 1L162618AH80
11. CONTROLLING OFFICE NAME AND ADDRESS US Army Armament Research and Development Command US Army Ballistic Research Laboratory (DRDAR-BL) Aberdeen Proving Ground, MD 21005		12. REPORT DATE July 1982
		13. NUMBER OF PAGES 52
14. MONITORING AGENCY NAME & ADDRESS (if different from Controlling Office)		15. SECURITY CLASS. (of this report) UNCLASSIFIED
		15a. DECLASSIFICATION/DOWNGRADING SCHEDULE
16. DISTRIBUTION STATEMENT (of this Report) Approved for public release; distribution unlimited.		
17. DISTRIBUTION STATEMENT (of the abstract entered in Block 20, if different from Report)		
18. SUPPLEMENTARY NOTES Supersedes BRL IMR 695 dated December 1980.		
19. KEY WORDS (Continue on reverse side if necessary and identify by block number) Intermediate Volatility Flight Stability Yawsonde		
20. ABSTRACT (Continue on reverse side if necessary and identify by block number) (1cb) Twelve yawsonde-instrumented, intermediate volatility agent (IVA) projectiles were tested at the BRL Transonic Range facility during August 1980. Two payload designs were tested. These 155mm prototype binary shell utilize a set of tandem, axially aligned canisters. The canisters are of different internal diameters, however. After rupture of the burst discs that separate the canisters, the interior geometry is not a simple cylinder as in the case of the 155mm M687 or the 8-inch XM736 binary projectiles. This unusual interior geometry cannot be easily analyzed for destabilizing effects of the liquid. Data from Charge 4 and		

DD FORM 1 JAN 78 1473 EDITION OF 1 NOV 65 IS OBSOLETE

UNCLASSIFIED

SECURITY CLASSIFICATION OF THIS PAGE (When Data Entered)

UNCLASSIFIED

SECURITY CLASSIFICATION OF THIS PAGE(When Data Entered)

20. ABSTRACT (Continued):

6 launches indicated stable flights for both canister designs. Previous tests at Dugway Proving Ground (DPG) had shown that one of the designs was unstable at Charge 4, but yawsondes were not employed so little information is available as to the nature of the unstable (or stable) flights. Since a reliable mathematical model is not available to aid in the design of the canister IVA configurations, additional testing must be conducted.

UNCLASSIFIED

SECURITY CLASSIFICATION OF THIS PAGE(When Data Entered)

# TABLE OF CONTENTS

	<u>Page</u>
LIST OF FIGURES . . . . .	5
LIST OF TABLES . . . . .	7
I. INTRODUCTION . . . . .	9
II. BACKGROUND . . . . .	9
III. HARDWARE DESCRIPTION . . . . .	10
IV. YAWSONDE DATA . . . . .	12
V. DISCUSSION AND CONCLUSIONS . . . . .	13
REFERENCES . . . . .	49
DISTRIBUTION LIST . . . . .	51

Accession For	
NTIS GRA&I	<input checked="" type="checkbox"/>
DTIC TAB	<input type="checkbox"/>
Unannounced	<input type="checkbox"/>
Justification	
By _____	
Distribution/	
Availability Codes	
Dist	Avail and/or Special
A	



**BLANK PAGE**

# LIST OF FIGURES

<u>Figure</u>		<u>Page</u>
1.	Cut-away View of a Standard XM736 Projectile, DT II Hardware . . . . .	15
2.	Cut-away View of the 155mm M687 Binary Projectile . . . . .	16
3.	Sigma-N versus Time (0-35 s) for Round 195B . . . . .	17
4.	Sigma-N versus Time (0-10 s) for Round 195B . . . . .	18
5.	Phi Dot (Raw) versus Time (0-35 s) for Round 195B . . . . .	19
6.	Sigma-N versus Time (0-35 s) for Round 187A . . . . .	20
7.	Sigma-N versus Time (0-10 s) for Round 187A . . . . .	21
8.	Phi Dot (Raw) versus Time (0-35 s) for Round 187A . . . . .	22
9.	Sigma-N versus Time (0-35 s) for Round 194B . . . . .	23
10.	Sigma-N versus Time (0-10 s) for Round 194B . . . . .	24
11.	Phi Dot (Raw) versus Time (0-35 s) for Round 194B . . . . .	25
12.	Sigma-N versus Time (0-30 s) for Round 186A . . . . .	26
13.	Sigma-N versus Time (0-10 s) for Round 186A . . . . .	27
14.	Phi Dot (Raw) versus Time (0-30 s) for Round 186A . . . . .	28
15.	Sigma-N versus Time (0-35 s) for Round 193B . . . . .	29
16.	Sigma-N versus Time (0-10 s) for Round 193B . . . . .	30
17.	Phi Dot (Raw) versus Time (0-35 s) for Round 193B . . . . .	31
18.	Sigma-N versus Time (0-35 s) for Round 185A . . . . .	32
19.	Sigma-N versus Time (0-10 s) for Round 185A . . . . .	33
20.	Phi Dot (Raw) versus Time (0-35 s) for Round 185A . . . . .	34
21.	Sigma-N versus Time (0-35 s) for Round 192B . . . . .	35
22.	Sigma-N versus Time (0-10 s) for Round 192B . . . . .	36
23.	Phi Dot (Raw) versus Time (0-35 s) for Round 192B . . . . .	37
24.	Sigma-N versus Time (0-35 s) for Round 184A . . . . .	38

# LIST OF FIGURES (Continued)

<u>Figure</u>		<u>Page</u>
25.	Sigma-N versus Time (0-10 s) for Round 184A . . . . .	39
26.	Phi Dot (Raw) versus Time (0-35 s) for Round 184A . . . . .	40
27.	Sigma-N versus Time (10-70 s) for Round 189B . . . . .	41
28.	Phi Dot (Raw) versus Time (10-70 s) for Round 189B . . . . .	42
29.	Sigma-N versus Time (10-70 s) for Round 181A . . . . .	43
30.	Phi Dot (Raw) versus Time (10-70 s) for Round 181A . . . . .	44
31.	Sigma-N versus Time (0-25 s) for Round 191B . . . . .	45
32.	Phi Dot (Raw) versus Time (0-25 s) for Round 191B . . . . .	46
33.	Sigma-N versus Time (0-25 s) for Round 183A . . . . .	47
34.	Phi Dot (Raw) versus Time (0-25 s) for Round 183A . . . . .	48



## LIST OF TABLES

<u>Table</u>		<u>Page</u>
1.	Physical Characteristics of 155mm Binary Shell . . . . .	10
2.	Round-By-Round Summary . . . . .	11

**BLANK PAGE**

## I. INTRODUCTION

A series of flight tests were conducted to determine the stability of two prototype designs for the 155mm intermediate volatility agent (IVA) binary projectile. Twelve shell with yawsondes were fired at transonic and supersonic launch conditions. All shell were stable. The liquid canister designs for these prototypes were unusual in that the forward and aft canisters were of different internal diameters and this geometry is presently not amenable to stability analyses for the liquid. Designs such as these must be carefully tested.

## II. BACKGROUND

Two previously developed binary projectiles, the 155mm M687 and the 8-inch XM736, both employed tandem canisters that were of the same internal diameters. A cut-away view of the XM736 is shown in Figure 1. Upon launch, the burst discs are ruptured and the resulting internal geometry seen by the liquid payload is essentially that of a right circular cylinder. The canister geometries for both the M687 and the XM736 were selected using the concepts of the Stewartson-Wedemeyer theory.<sup>1,2</sup> This theory determines the liquid moments and eigenfrequencies for a wholly or partially filled cylinder. The analysis considers viscous effects and the stability of the liquid/projectile system when the liquid is rotating as a rigid body. Instability will occur if one of the liquid eigenfrequencies is close to the fast precessional mode (nutational frequency) of the projectile. The eigenfrequencies principally depend upon the liquid fill ratio and the cylinder aspect ratio (height/diameter). For the IVA geometry a simple aspect ratio cannot be defined, hence the Stewartson-Wedemeyer theory cannot be directly applied.

Prior to the yawsonde-instrumented flights, laboratory tests were conducted with a liquid-filled gyroscope to examine the use of an average aspect ratio.<sup>3</sup> An average radius ( $\bar{a}$ ) can be determined using the height ( $2c$ ) and the total volume of the cylinder ( $V_T$ ),

---

<sup>1</sup>K. Stewartson, "On the Stability of a Spinning Top Containing Liquid," J. Fluid Mech., Vol. 5, Part 4, September 1959, pp. 577-592.

<sup>2</sup>E.H. Wedemeyer, "Viscous Corrections to Stewartson's Stability Criterion," BRL Report No. 1325, Aberdeen Proving Ground, Maryland, June 1966. AD 489687.

<sup>3</sup>William P. D'Amico, Jr. and Michael D. Fuller, "Experimental Study of a Liquid-Filled Cylinder with Unequal Internal Diameters," BRL Memorandum Report in publication.

$$\bar{a} = (V_T/2c\pi)^{1/2}$$

The average aspect ratio was then defined as  $c/\bar{a}$ , and it was used to implement the Stewartson-Wedemeyer theory. Theoretical predictions were then compared to the gyroscope data, and it was determined that the average aspect ratio theory and the data were not consistent. The use of the average aspect ratio concept would produce uncertainty within a projectile design.

Liquid-induced instabilities of the Stewartson-Wedemeyer type are common during spin-up, but only a model for prediction of the liquid eigenfrequencies exists. No estimation of the destabilizing liquid moment during spin-up is available. Spin-up eigenfrequency histories were computed in Reference (3), but the differences between the two designs were quite small and no qualitative arguments could be made as to why one design should be stable while the other should be unstable.

### III. HARDWARE DESCRIPTION

A cut-away view of the M687 projectile is shown in Figure 2. The projectile metal parts for the 155mm IVA shell will be those of an M687, but a new set of canisters will be employed. Table 1 lists the physical dimensions of the standard M687 and the two IVA prototypes.

Table 1. Physical Characteristics of 155mm Binary Shell\*

Projectile Type	Mass (kg)	Moments of Inertia		Top Canister		Rear Canister		$c/\bar{a}$
		$I_x$ (kg·m <sup>2</sup> )	$I_y$ (kg·m <sup>2</sup> )	L (cm)	D(cm)	L(cm)	D(cm)	
M687	41.95	0.1617	1.767	19.30	10.74	28.57	10.74	4.457
Model A	45.12	0.1733	1.691	15.85	10.80	34.46	11.11	4.469
Model B	46.17	0.1728	1.841	16.84	10.80	32.95	11.43	4.438

\*Measurements taken with filled canisters.

For yaw induced launches at Charge 4, Model A was unstable when tested at DPG. Yawsondes were not employed, hence the details of these flights are not available. It is highly possible that poor flight performance for Model A occurred prior to liquid spin-up. Upon launch, the liquid is not rotating. During the down range flight, however, the liquid is spun-up by the projectile. This transfer of angular momentum can be seen in yawsonde determined spin histories as a rapid decrease in the projectile rotation rate at shot exit. Normally this rapid despin is observed for about one second, but theoretical predictions of liquid

spin-up and the associated projectile spin-decay indicate that the spin-up process can encompass a large portion of the total time of flight (for a Charge 4-30 second time of flight, an M687 can take 15 seconds to achieve 90 percent of the angular momentum of an equivalent frozen liquid payload).<sup>4</sup>

Table 2 gives a round-by-round history of the test program. A three digit number which was stamped on the projectile was augmented with an A or a B to denote model type. An M109A1 vehicle was used to launch the projectiles. A standard muzzle break was used for Charge 6 launches, while a modified muzzle break (12.7 cm side plates) was used to induce yaw at Charge 4. A muzzle chronograph was used to measure launch velocities (velocities shown in the table have not been corrected back to the muzzle). Time-zero measurements were made using a strain gage attached to the tube.

Table 2. Round-By-Round Summary

CSL Number <sup>a</sup>	BRL Number	Firing Date	Muzzle Velocity (m/s)	FMA <sup>b</sup> (degrees)	Quadrant Elevation (degrees)	Launch Condition <sup>c</sup>
195B	1626	27 Aug 80	336.2	9.5	30	Chg 4/YI
187A	1627	27 Aug 80	349.0	9.5	30	Chg 4/YI
194B	1720	27 Aug 80	338.3	9.5	30	Chg 4/YI
186A	1721	27 Aug 80	337.4	8.5	30	Chg 4/YI
193B	1718	28 Aug 80	334.4	12.5	30	Chg 4/YI
185A	1713	28 Aug 80	339.5	12	30	Chg 4/YI
192B	1714	28 Aug 80	336.8	11.5	30	Chg 4/YI
184A	1715	28 Aug 80	340.5	8	30	Chg 4/YI
189B	1624	28 Aug 80	458.4	----	67	Chg 6
181A	1625	28 Aug 80	462.1	----	67	Chg 6
191B	1716	28 Aug 80	460.9	3	17	Chg 6
183A	1697	28 Aug 80	463.3	----	17	Chg 6

<sup>a</sup>A-type shell contained canisters with a 0.793 cm (5/16 inch) wall thickness, while B-type shell had 0.635 cm (1/4 inch) wall canisters.

<sup>b</sup>FMA is defined as the first maximum angle of yaw and is determined as half of the first peak-to-peak excursion in Sigma N. FMA is taken only as a measure of the first maximum yaw level.

<sup>c</sup>Yaw induction (YI) with a modified muzzle brake with full (12.7 cm) side plates.

<sup>4</sup>C.W. Kitchens, Jr. and N. Gerber, "Prediction of Spin-Decay of Liquid-Filled Projectiles," Ballistic Research Laboratories Report No. 1996, July 1977. AD A043275.

Yawsondes configured in the shape of a standard artillery fuze were installed on the test projectiles.<sup>5</sup> Yawsonde data provide a planar view of the angular motion of the projectile during flight. The angular motion is shown in terms of Sigma N which is the complement of an angle between a vector to the sun and the roll axis of the projectile. Sigma N will vary along the trajectory, but peak-to-peak excursions in Sigma N provide the amplitude of the yawing motion about the trajectory. The spin of the projectile is presented in terms of Phi Dot (Raw), which is the derivative with respect to time of the Eulerian roll angle Phi. For large angular motions, the Phi Dot (Raw) history will exhibit oscillations. The mean of these oscillations should be considered to be the spin.<sup>6</sup> Spin will normally be used in place of the terminology Phi Dot (Raw) in this report.

#### IV. YAWSONDE DATA

Four rounds fired on 27 August 1980 were launched at Charge 4 with yaw induction. Round 195B was launched with an FMA of 9.5 degrees and was stable (Figures 3 and 4). The fast mode precession damped to less than 2 degrees of peak-to-peak motion by 10 seconds. The spin history shown in Figure 5 was normal. The oscillations on the spin history during the first 5 seconds are produced by the large angular motion that was induced at launch. The effects of the large angular motion on the spin history during the first several seconds cloud the rapid despin of the projectile during the liquid spin-up stage. The second test projectile, Round 187A, had an FMA level similar to the first round. The motion was stable and the fast mode precession was again damped by 10 seconds (Figures 6 and 7). Spin data are shown in Figure 8. The next shell (Round 194B) exhibited behavior similar to the first rounds (Figures 9, 10, and 11). The Sigma N data at 0.75 seconds were apparently clipped. However, the data during the next cycle of the motion were normal. Figures 12 and 13 give the angular motion for Round 186A. An FMA of only 8.5 degrees was observed. The spin history is shown in Figure 14 and was normal.

---

<sup>5</sup>W.H. Mermagen and W.H. Clay, "The Design of a Second Generation Yawsonde," Ballistic Research Laboratories Memorandum Report No. 2368, April 1974. AD 780064.

<sup>6</sup>C.H. Murphy, "Effect of Large High-Frequency Angular Motion of a Shell on the Analysis of Its Yawsonde Records," Ballistic Research Laboratory Memorandum Report No. 2581, February 1976. AD B009421L.

A second series of test rounds were launched at Charge 4 with yaw induction on 28 August 1980. The same gun and yaw inducer were used as on the previous day, but slightly higher yaw levels were achieved. The angular motion for Round 193B is on Figures 15 and 16 (FMA of 12.5 degrees). The spin history for this shell (Figure 17) clearly shows a rapid despin of the projectile during the first second of flight as the liquid is being spun-up. Data for the next projectile (Round 185A) are shown in Figures 18, 19, and 20. An FMA level similar to Round 193B was achieved. Figures 21, 22, and 23 give the angular motion and spin histories for Round 192B. An FMA of 11.5 degrees was produced, which was slightly smaller than the two previous rounds. This round was stable with no abnormal behavior. The last round fired at Charge 4 was Round 184A. Data for this round are shown in Figures 24, 25, and 26. This shell had the smallest FMA of any of the rounds within this group, 8 degrees.

On 28 August 1980, shells were also launched at Charge 6. The first two rounds were launched at a quadrant elevation of 67 degrees. The yawsondes were out of view of the sun during the early portions of the trajectories due to the high quadrant elevation, but good data were obtained over the remainder of the flight paths. Data for Round 189B are shown in Figures 27 and 28, while data for Round 181A are shown in Figures 29 and 30. No unusual motions were observed. The final two rounds were launched at a quadrant elevation of 17 degrees, and both shells were stable. The first projectile (Round 191B) had an FMA of 3 degrees. The launch disturbances decayed within 3 seconds and almost no angular motion was evident until the limit cycle behavior returned at 10 seconds (Figure 31). Figure 32 clearly shows the rapid despin of the projectile during the first second of flight. The spin decay during the rest of the flight was dominated by air friction over the projectile. Little data were obtained from the last round of the test program (Round 183A) since the yawsonde was not in view of the sun for the entire trajectory. Available data are shown in Figures 33 and 34, and no unusual behavior was observed.

## V. DISCUSSION AND CONCLUSIONS

The yawsonde data gave no indication that either the A or B designs would be unstable. This was not expected, since previous testing at DPG had shown the A configuration to be unstable. Past experiences at DPG with 155mm liquid-filled shells have shown yaw levels similar to those achieved during this test. An important difference is the high altitude at DPG, which would reduce aerodynamic damping due to the low atmospheric density conditions. The tests at the Transonic Range facility were of course essentially at sea level and high humidity/high density conditions. If the stable or unstable flight performance of the A model is attributed to differences in atmospheric density, then the projectile must be considered to be marginally stable. As to conclusions on the stability of the B model, very few can be made.

No unstable flights were observed during the present test sequence, but it would be recommended that yawsonde-instrumented flights be performed at DPG where the companion design was unstable.

The geometry of the proposed IVA payload canisters are not amenable to analysis by available liquid-filled shell theory. Uninstrumented flight tests at DPG demonstrated unstable flight behavior for a canister design with an average aspect ratio of 4.469, while stable flights occurred for a design with an average aspect ratio of 4.438. If the stability of a projectile is modified due to a change in aspect ratio of less than one percent, then the system is a very sensitive one. Without the aid of a rational mathematical model, such a sensitive shell design should be carefully and completely tested.



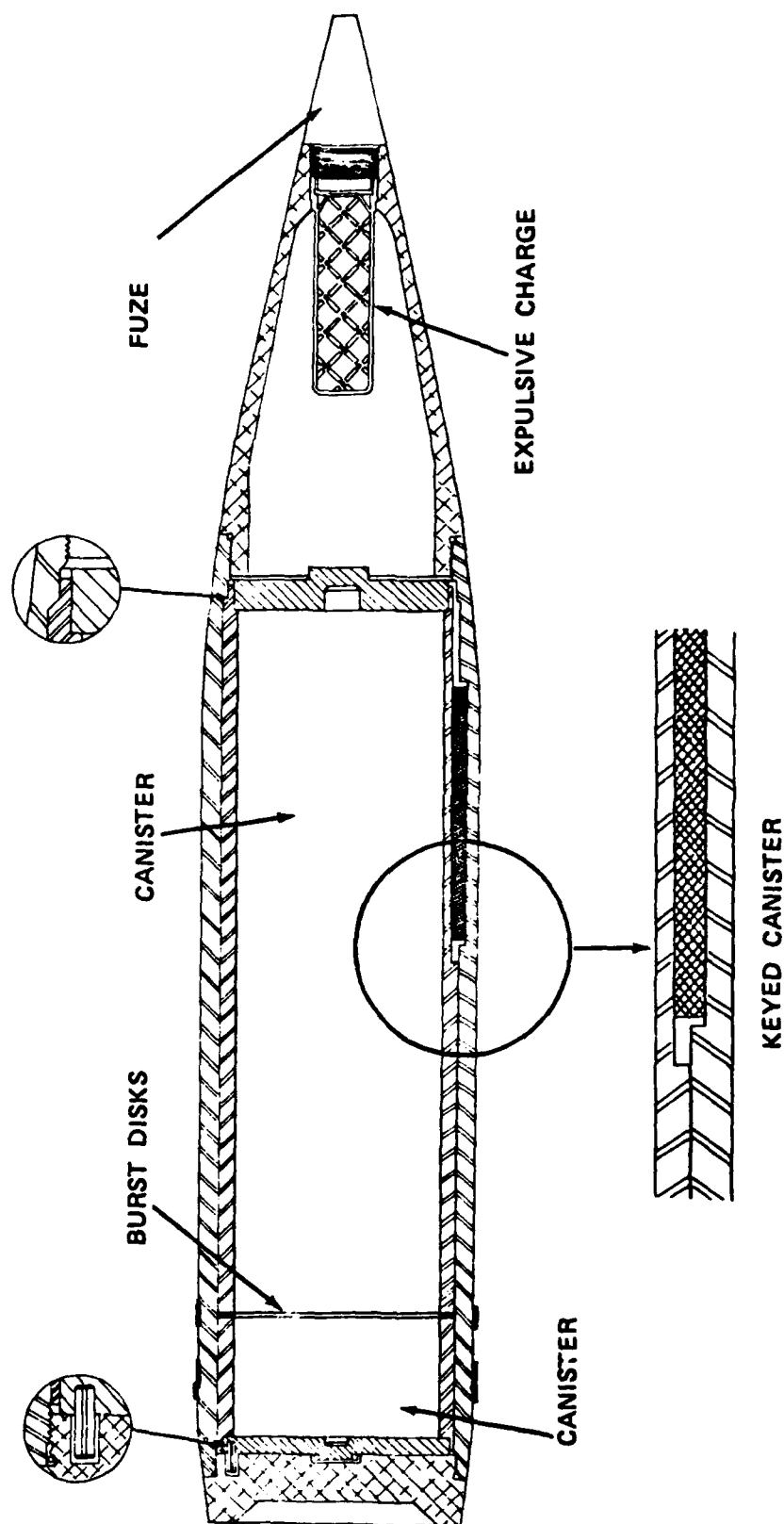


Figure 1. Cut-away view of a standard XM736 projectile, DT II hardware.

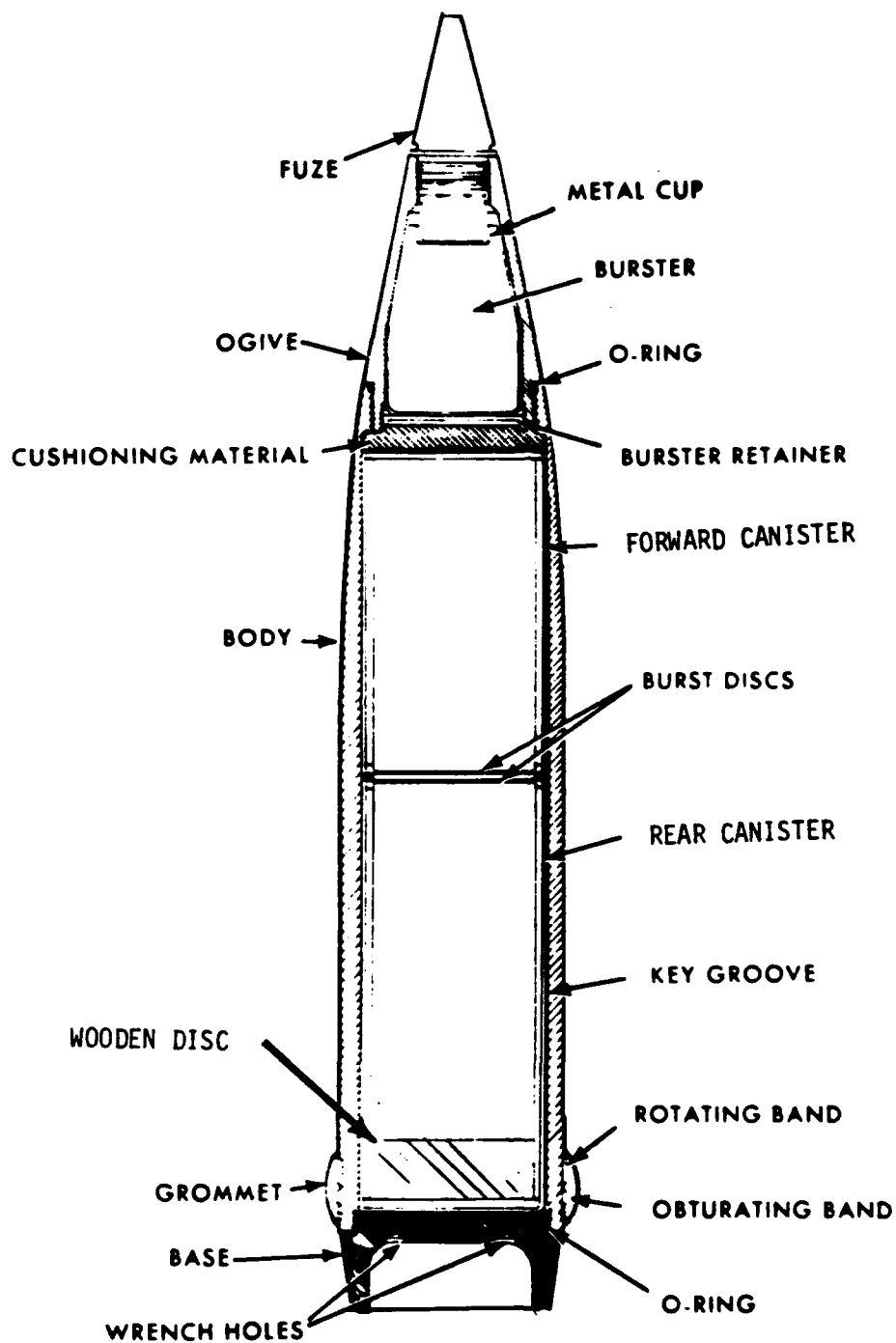


Figure 2. Cut-away view of the 155mm M687 binary projectile.

SITE I.D. CSL195B      BRL ROUND1626      FIRED      27AUG80

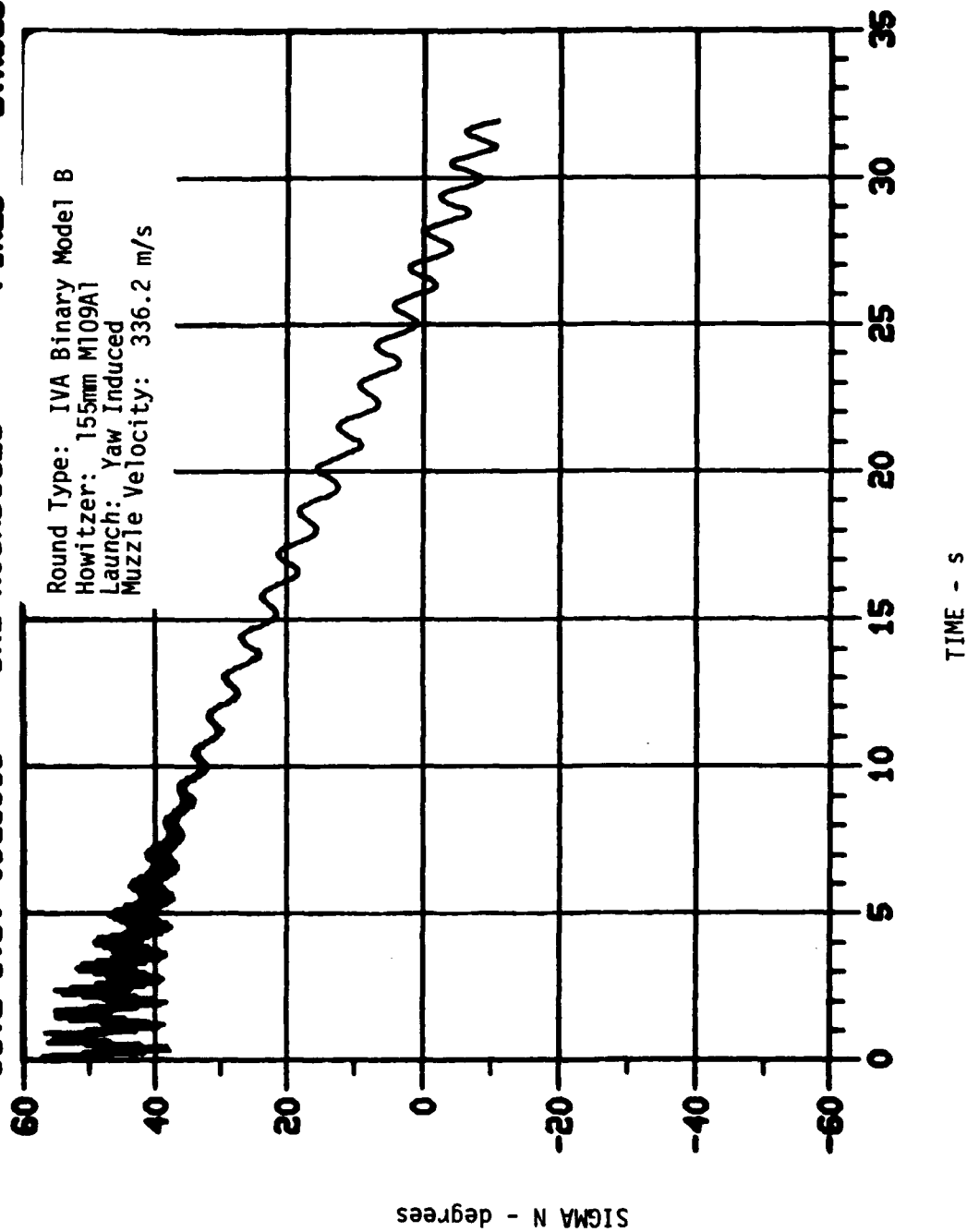


Figure 3. Sigma N versus Time (0-35 s) for Round 1958.

SITE I.D. CSL195B      BRL ROUND1626      FIRED      27AUG80

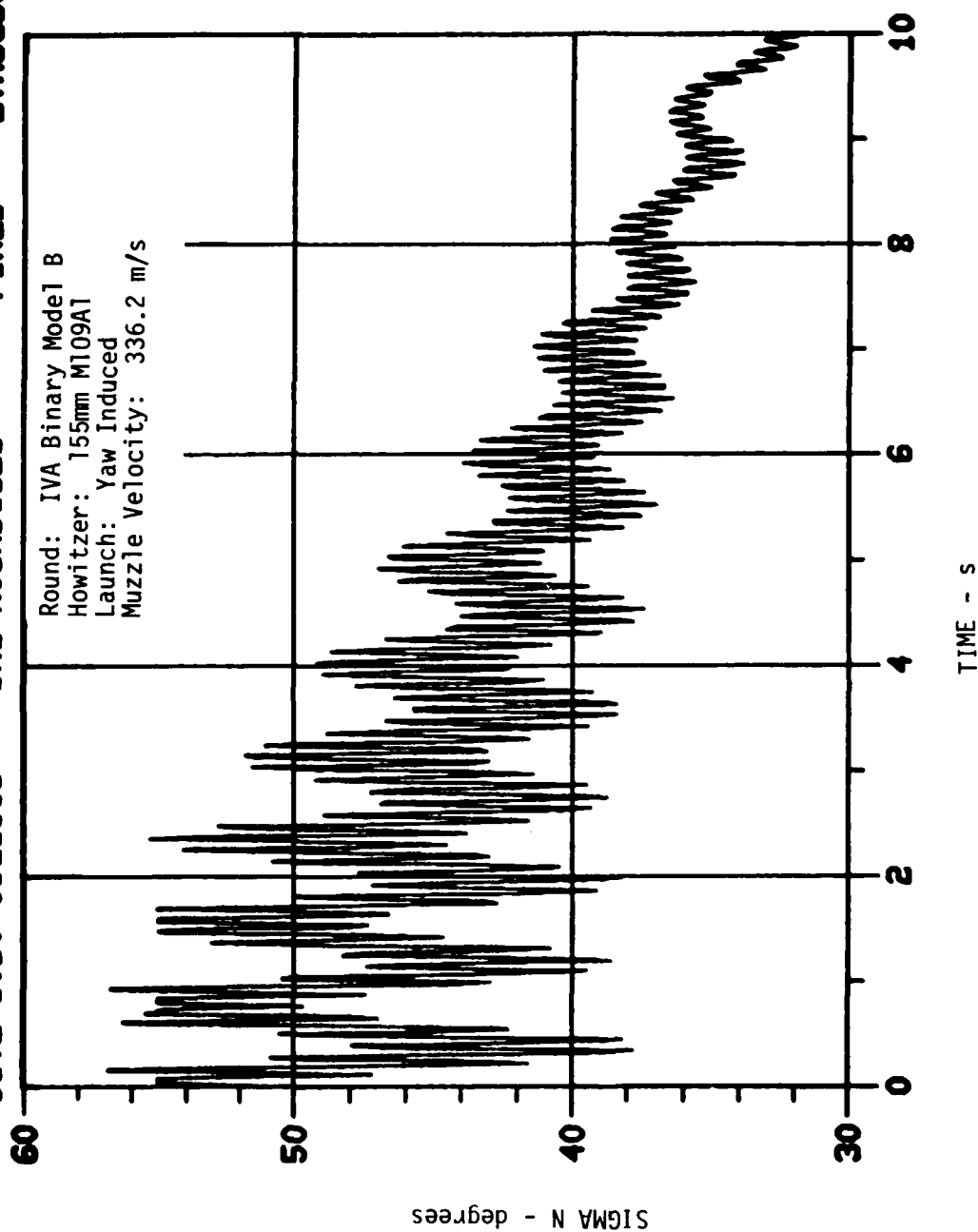


Figure 4. Sigma N versus Time (0-10 s) for Round 195B.

SITE I.D. CSL1958 BRL ROUND1626 FIRED 27AUG80

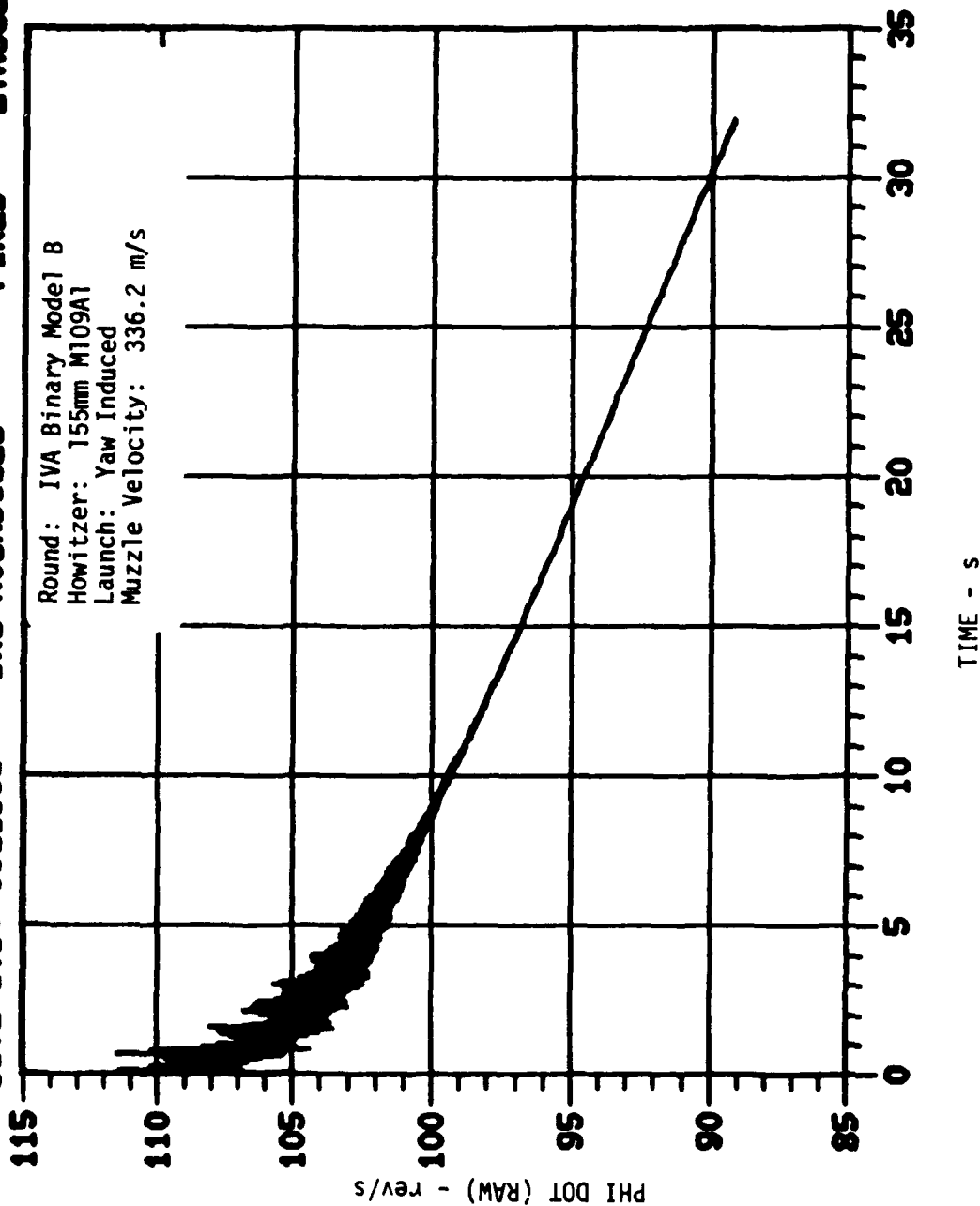


Figure 5. Phi Dot (Raw) versus Time (0-35 s) for Round 1958.

SITE I.D. CSL187A      BRL ROUND1627      FIRED      27AUG80

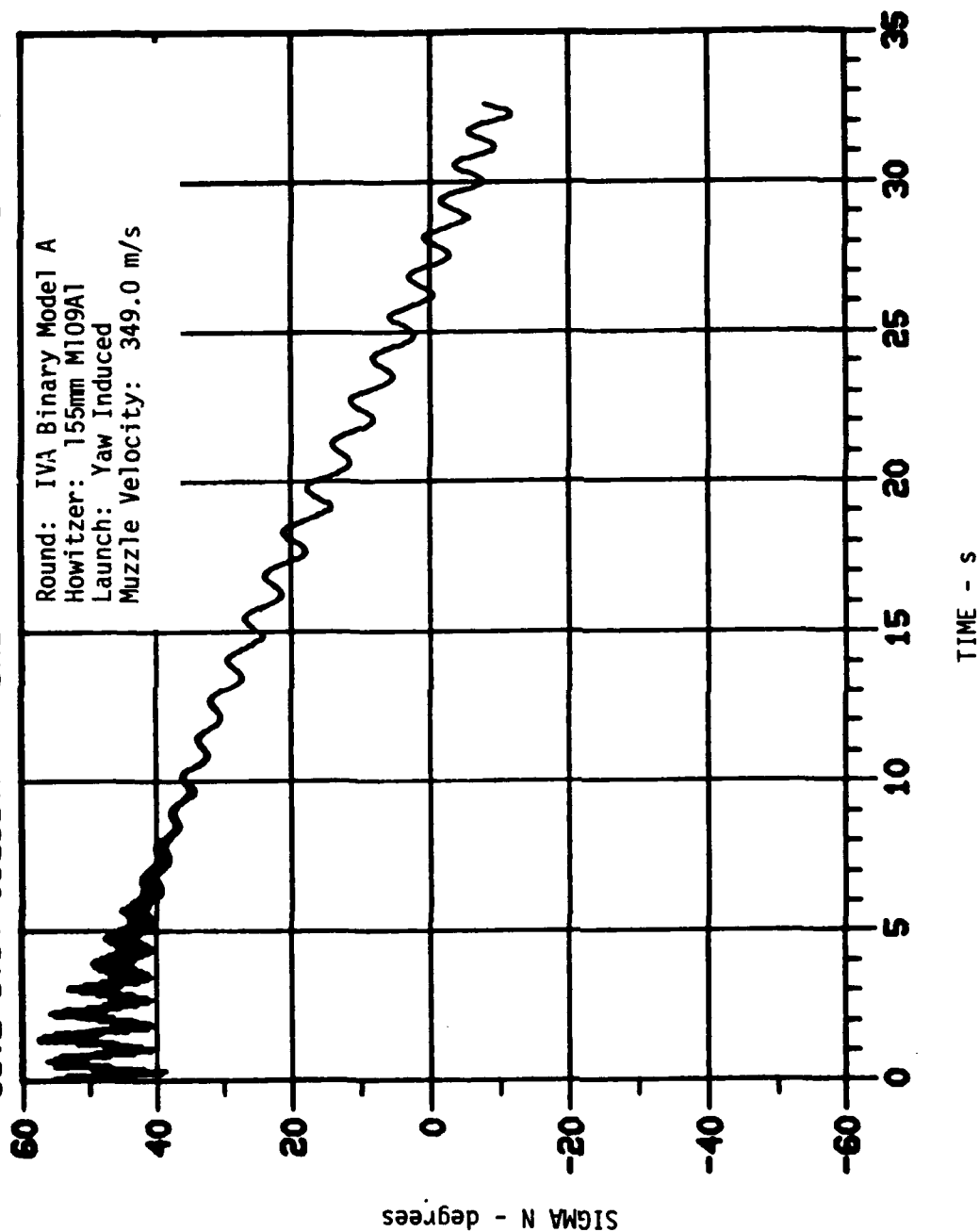


Figure 6. Sigma N versus Time (0-35 s) for Round 187A.

SITE I.D. CSL187A      BRL ROUND1627      FIRED      27AUG80

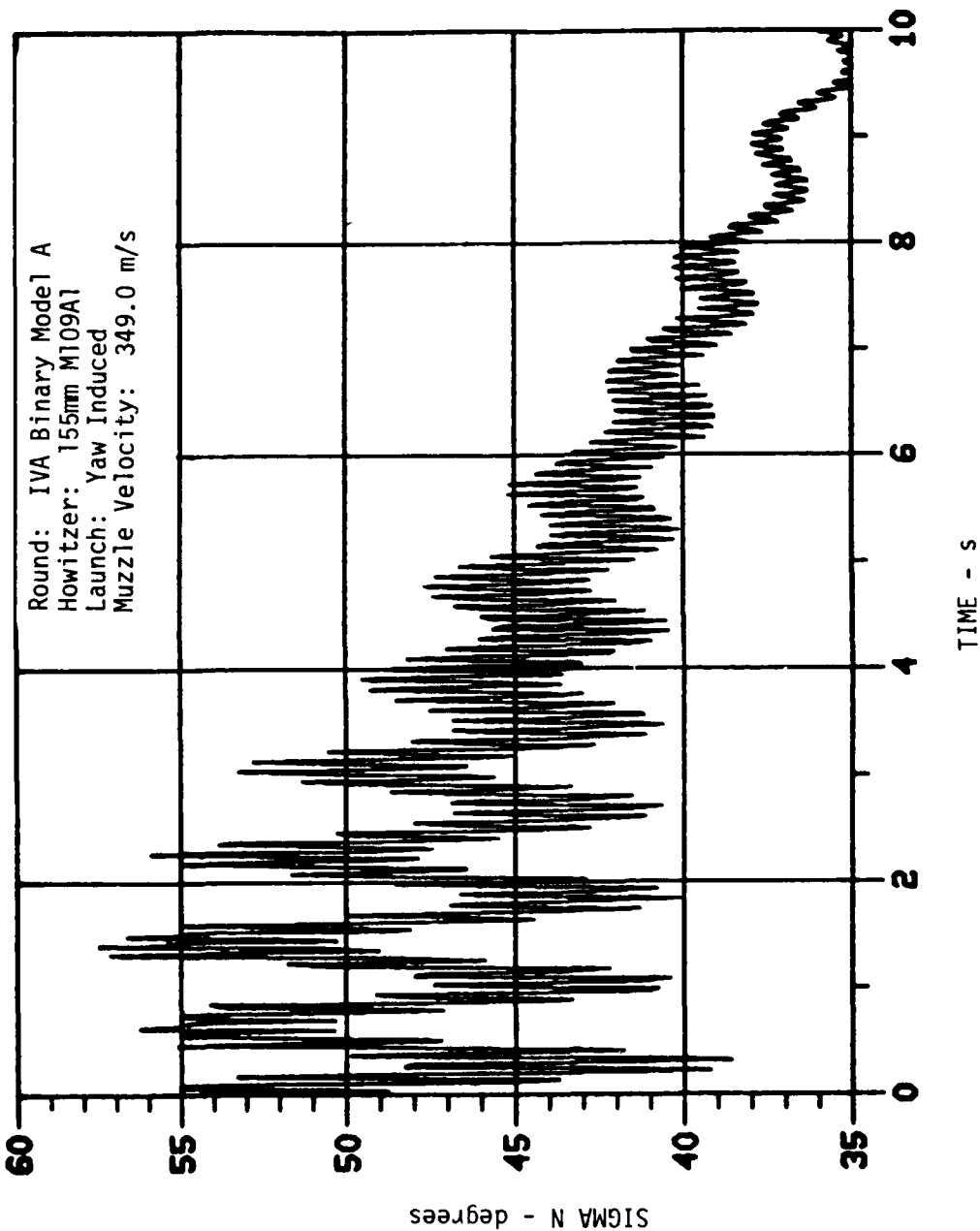


Figure 7. Sigma N versus Time (0-10 s) for Round 187A.

SITE I.D. CSL187A      BRL ROUND1627      FIRED      27AUG80

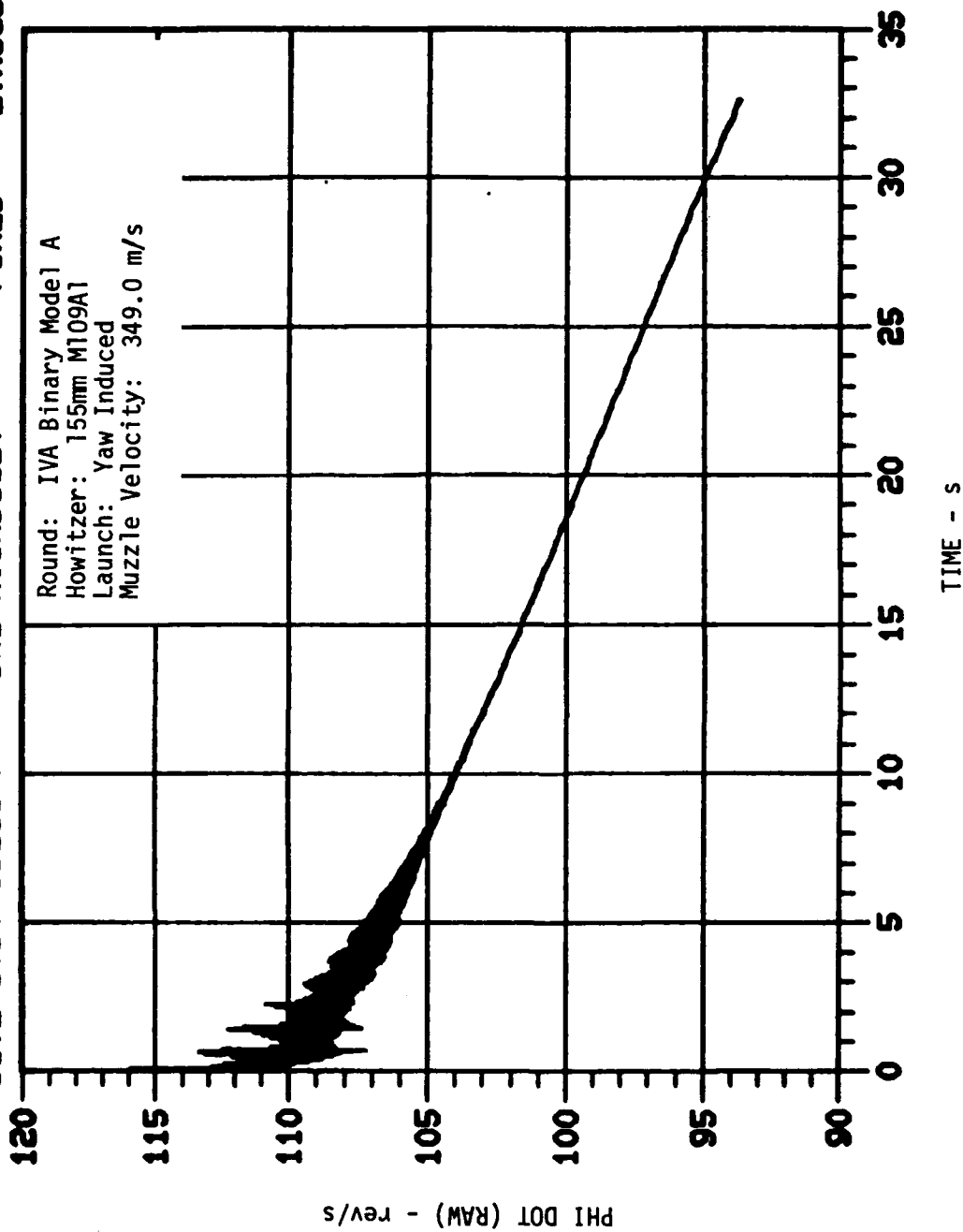


Figure 8. Phi Dot (Raw) versus Time (0-35 s) for Round 187A.



SITE I.D. CSL194B      BRL ROUND1720      FIRED      27AUG80

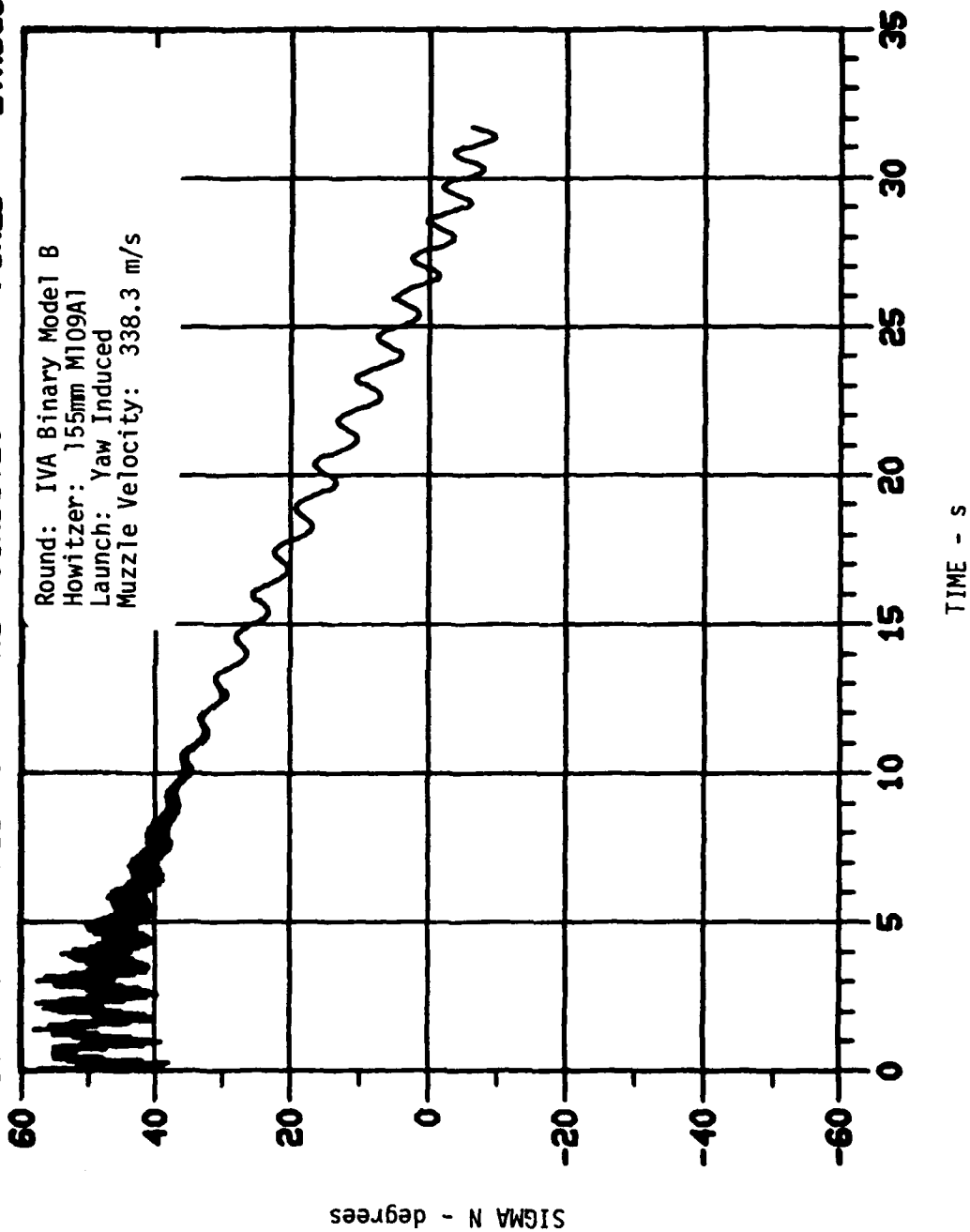


Figure 9. Sigma N versus Time (0-35 s) for Round 194B.

SITE I.D. CSL194B      BRL ROUND1720      FIRED      27AUG80

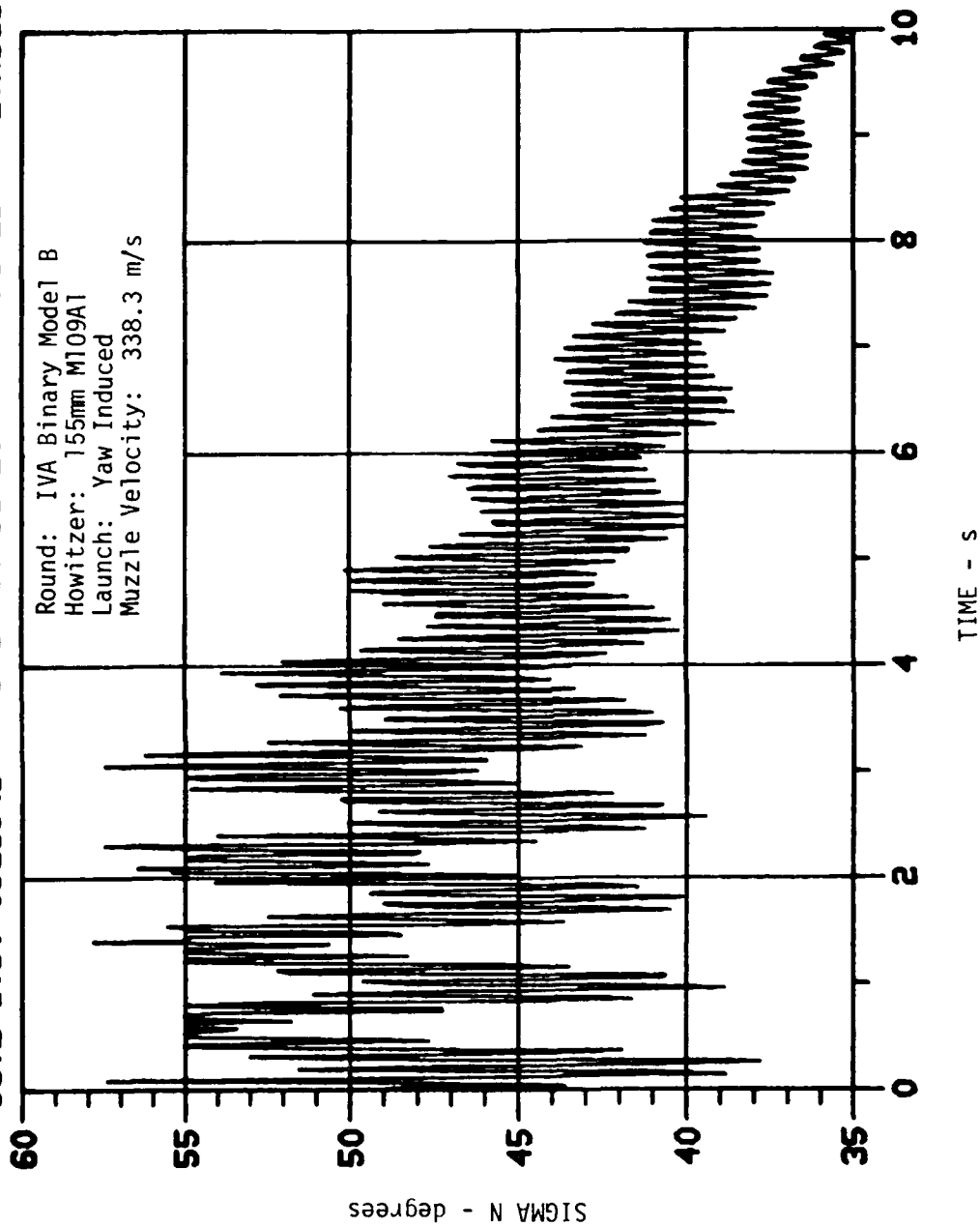


Figure 10. Sigma N versus Time (0-10 s) for Round 194B.

SITE I.D. CSL194B BRL ROUND1720 FIRED 27AUG80

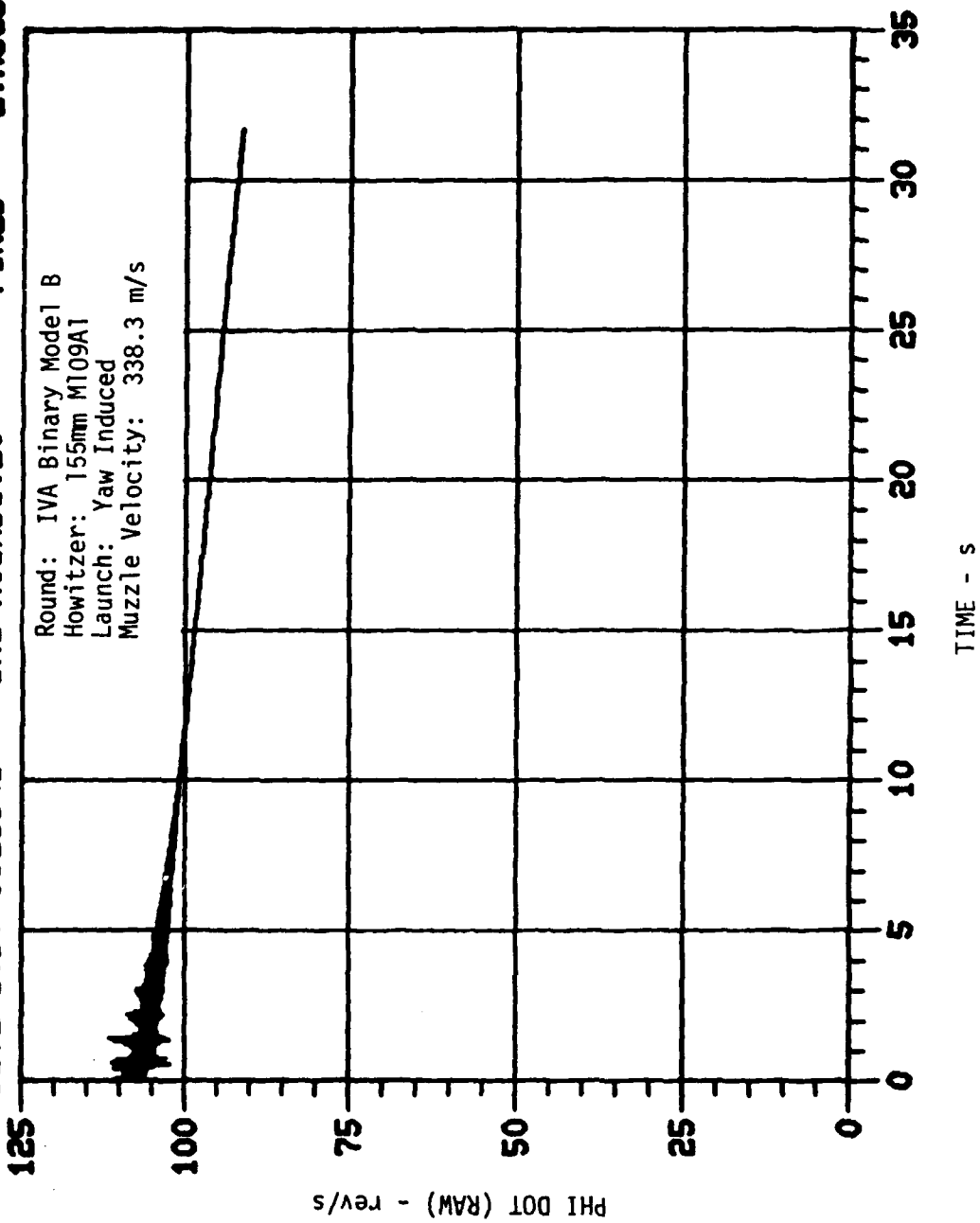


Figure 11. Phi Dot (Raw) versus Time (0-35 s) for Round 194B.

SITE I.D. CSL186A

BRL ROUND1721

FIRE

27AUG80

Round: IVA Binary Model A  
Howitzer: 155mm M109A1  
Launch: Yaw Induced  
Muzzle Velocity: 337.4 m/s

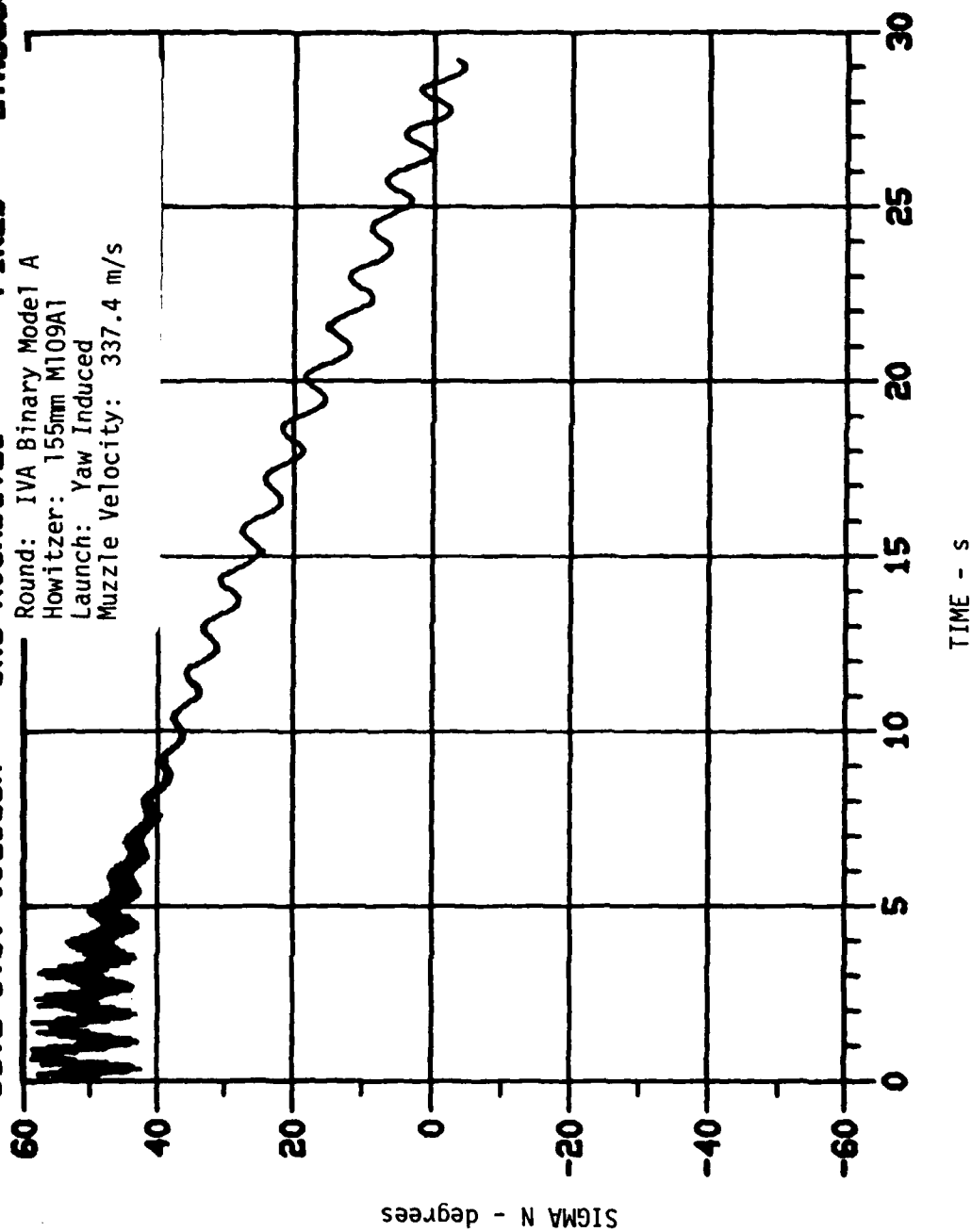


Figure 12. Sigma N versus Time (0-30 s) for Round 186A.

SITE I.D. CSL186A      BRL ROUND1721      FIRED      27AUG80

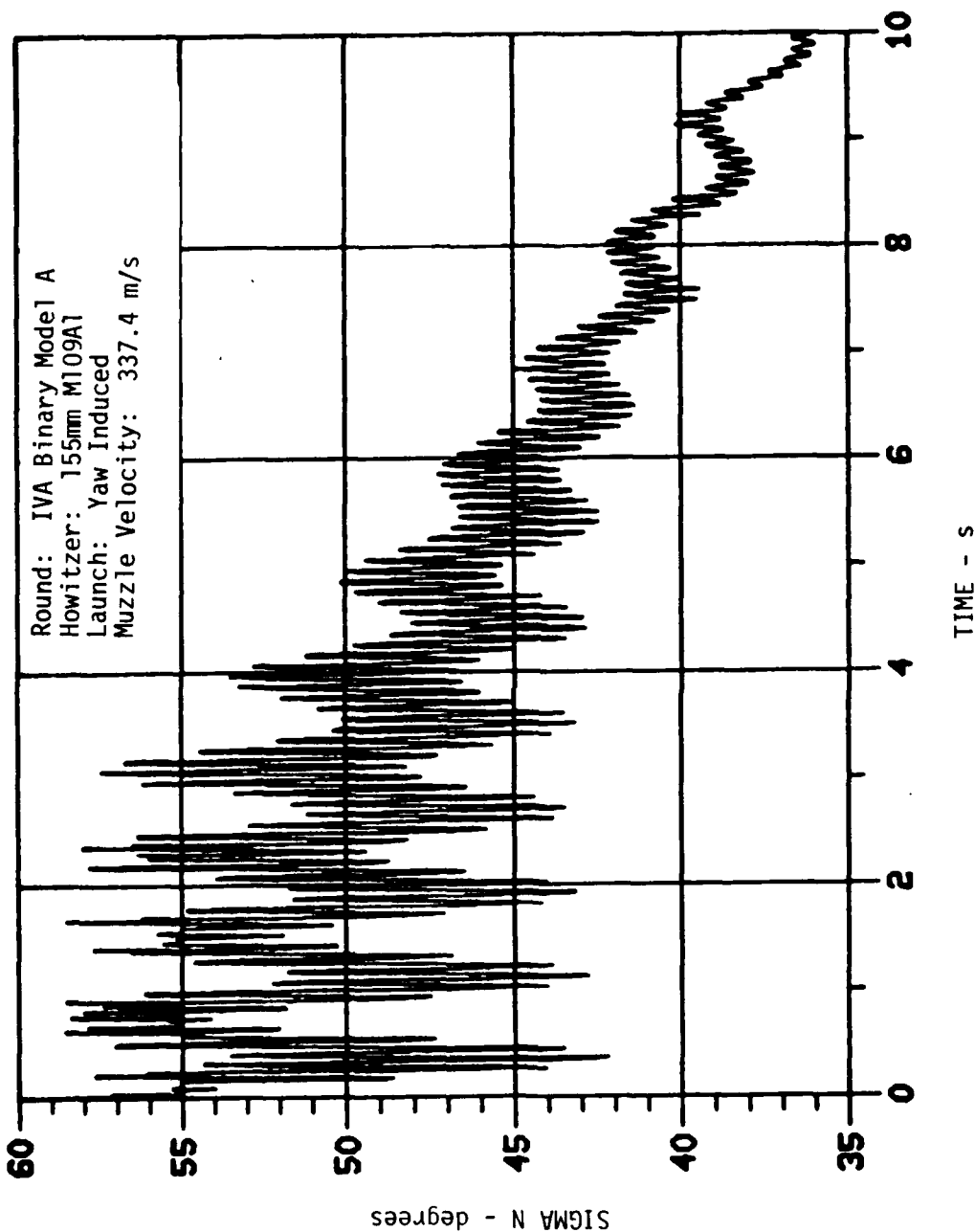


Figure 13. Sigma N versus Time (0-10 s) for Round 186A.

SITE I.D. CSL186A      BRL ROUND1721      FIRED      27AUG80

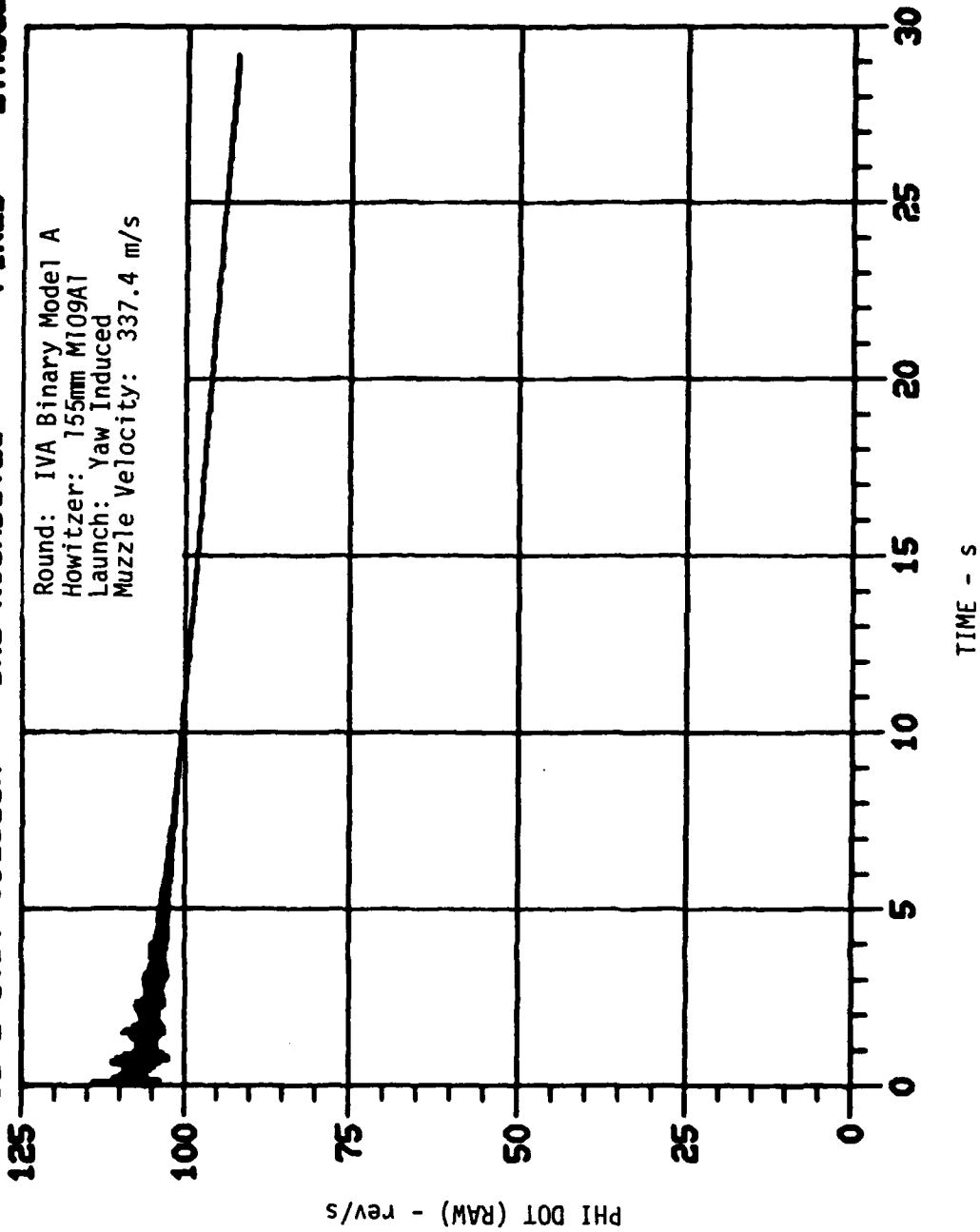


Figure 14. Phi Dot (Raw) versus Time (0-30 s) for Round 186A.

SITE I.D. CSL193B      BRL ROUND1718      FIRED      28AUG80

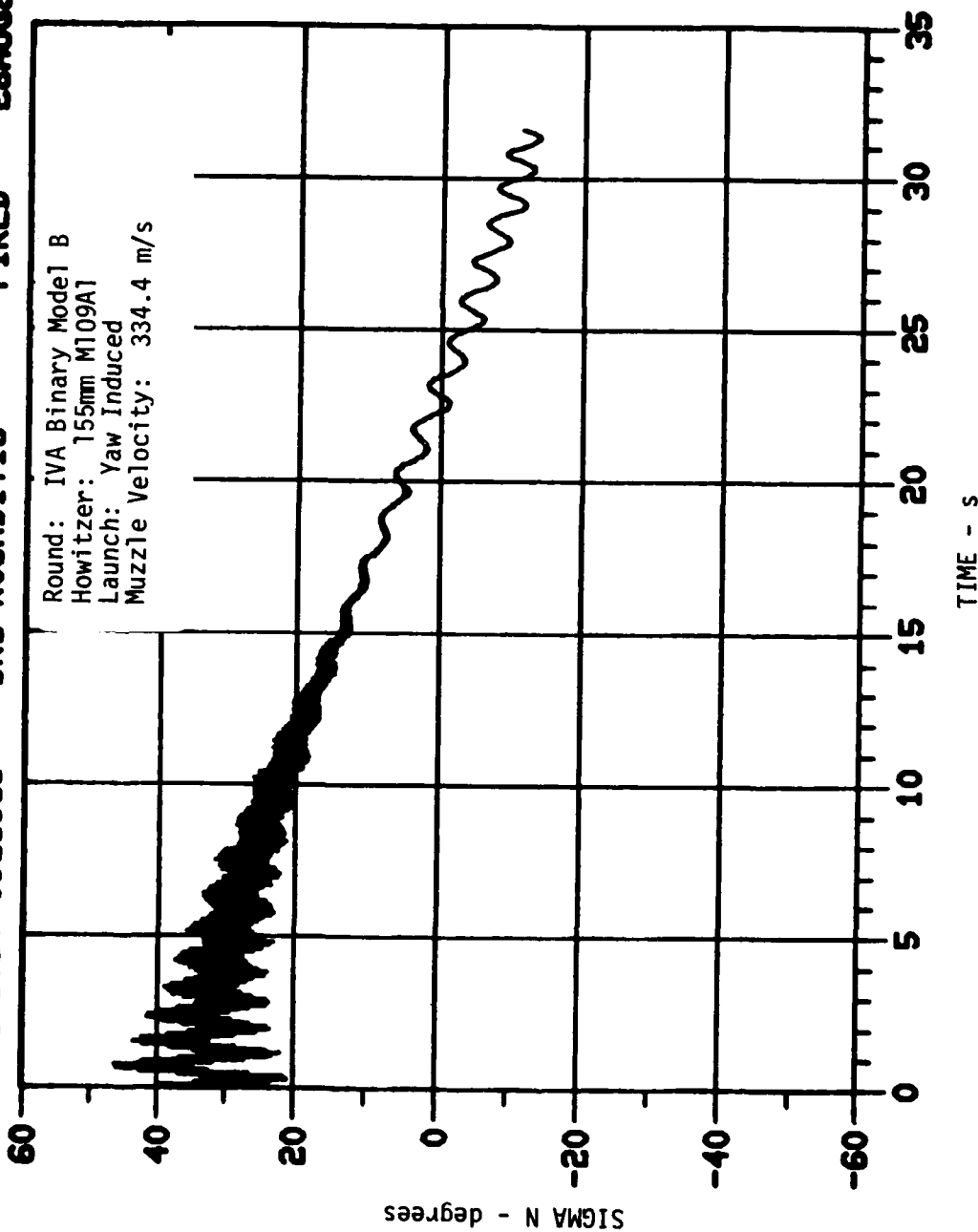


Figure 15. Sigma N versus Time (0-35 s) for Round 193B.

SITE I.D. CSL193B      BRL ROUND1718      FIRED      28AUG80

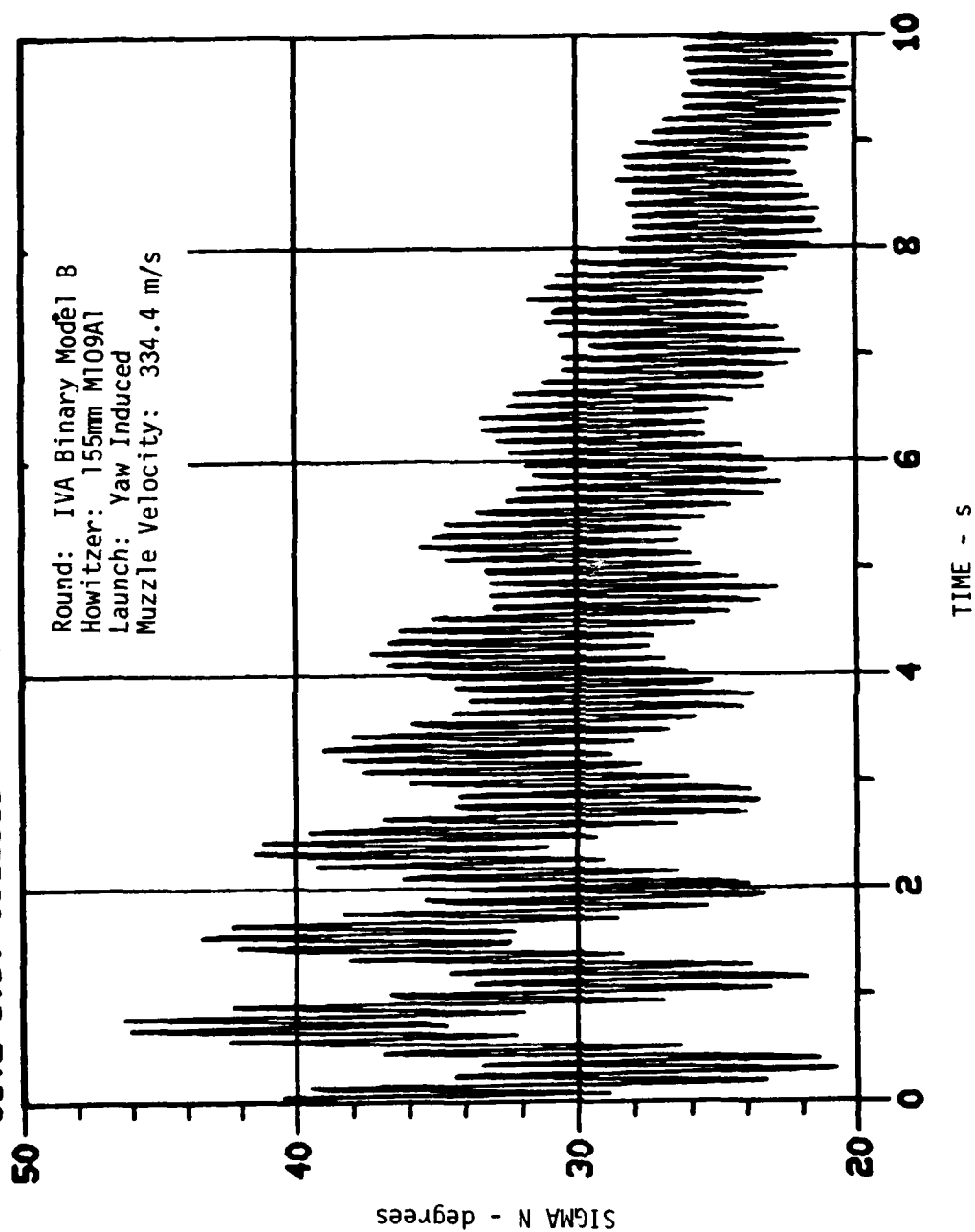


Figure 16. Sigma N versus Time (0-10 s) for Round 193B.



SITE I.D. CSL193B      BRL ROUND1718      FIRED      28AUG80

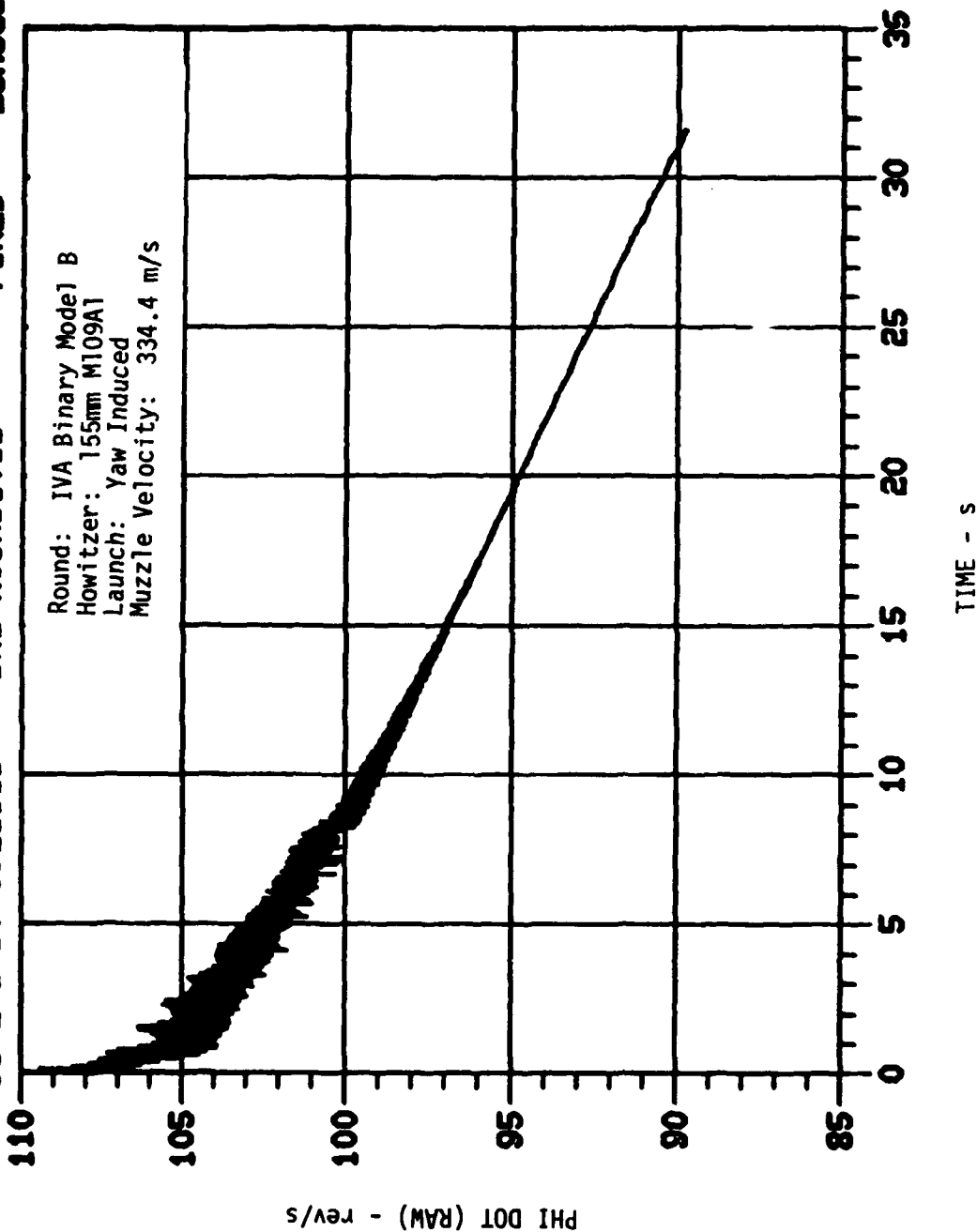


Figure 17. Phi Dot (Raw) versus Time (0-35 s) for Round 193B.

SITE I.D. CSL185A      BRL ROUND1713      FIRED      28AUG80

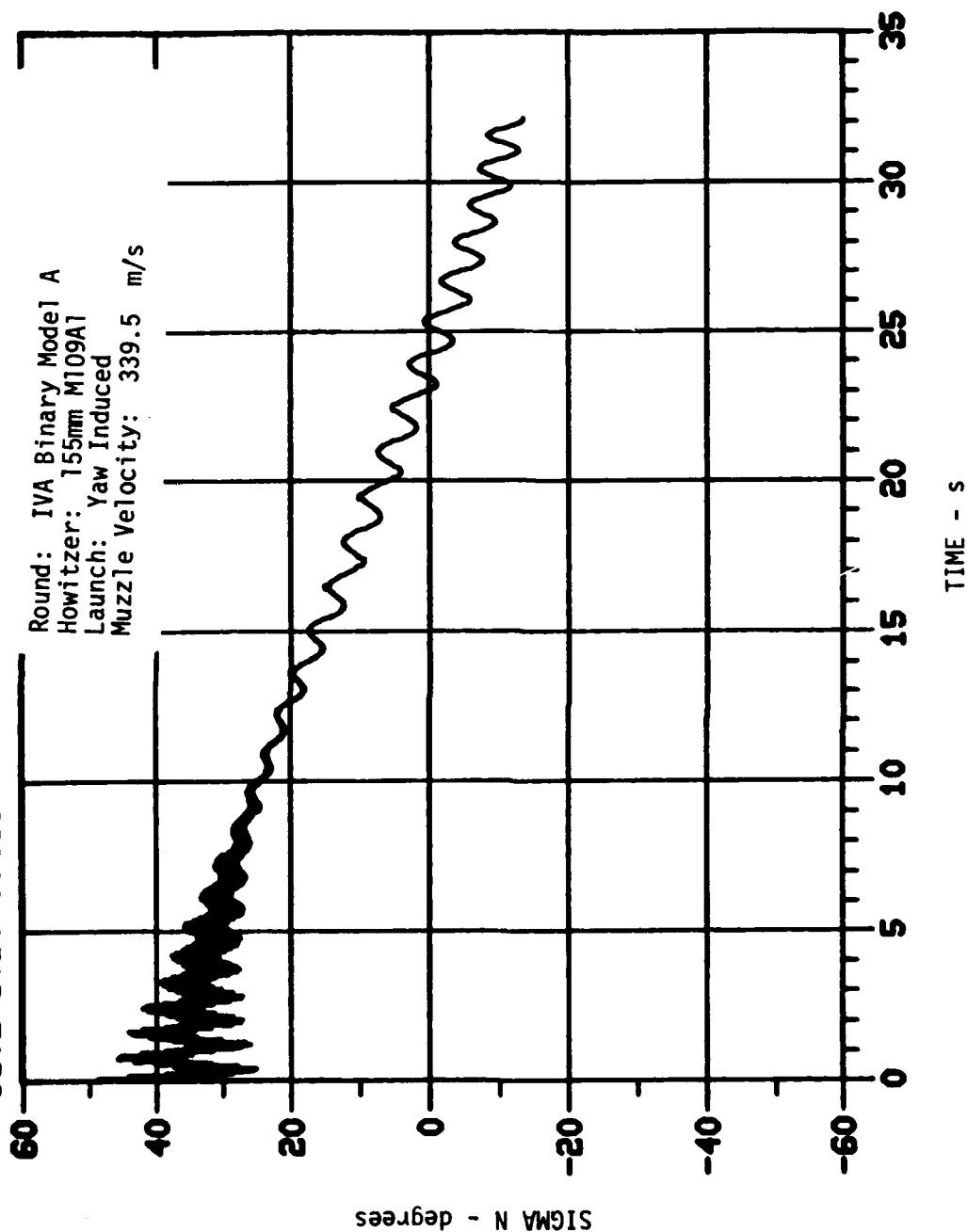


Figure 18. Sigma N versus Time (0-35 s) for Round 185A.

SITE I.D. CSL185A

BRL ROUND1713

FIRE

28AUG80

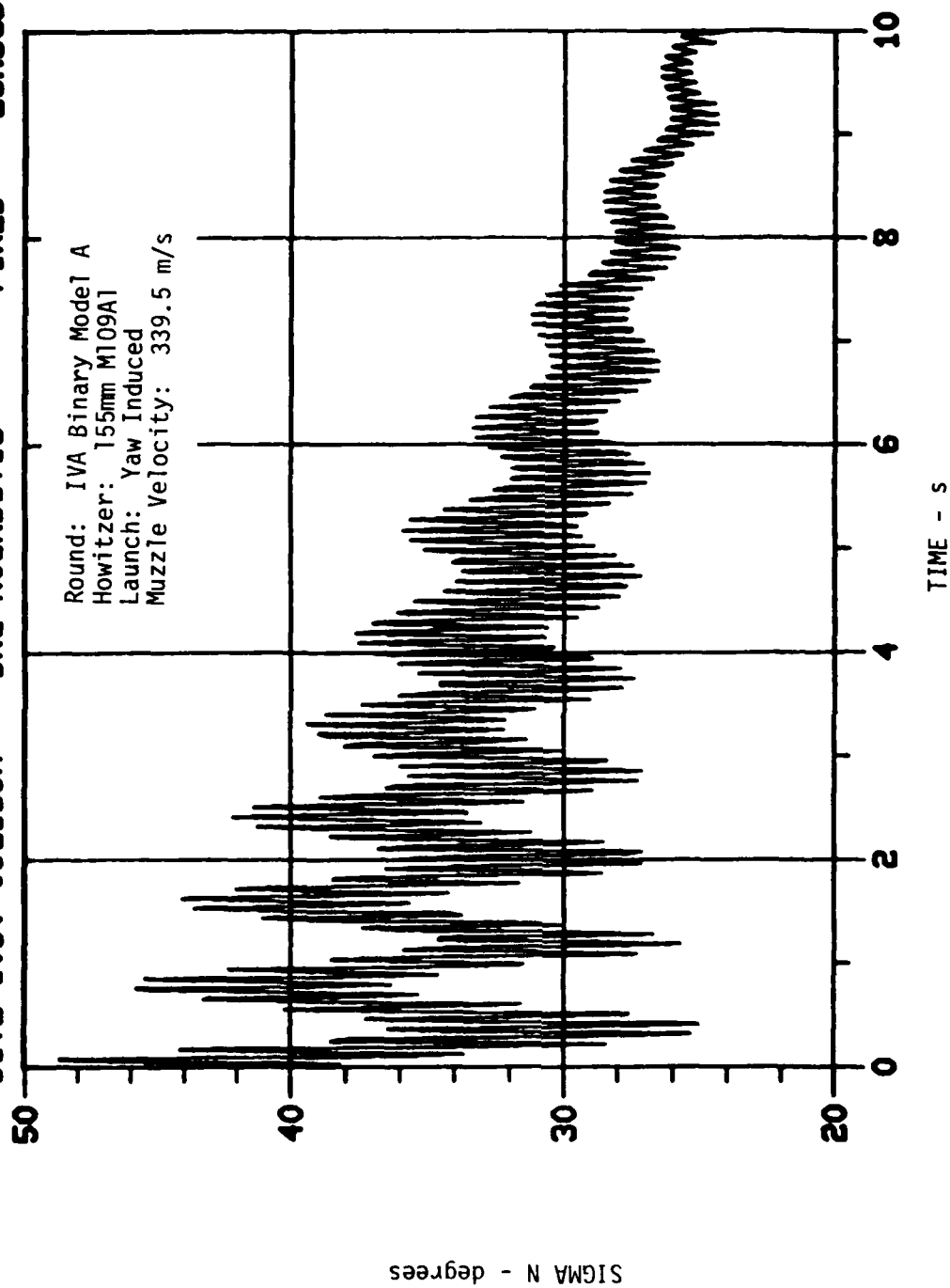


Figure 19. Sigma N versus Time (0-10 s) for Round 185A.

SITE I.D. CSL185A      BRL ROUND1713      FIRED      28AUG80

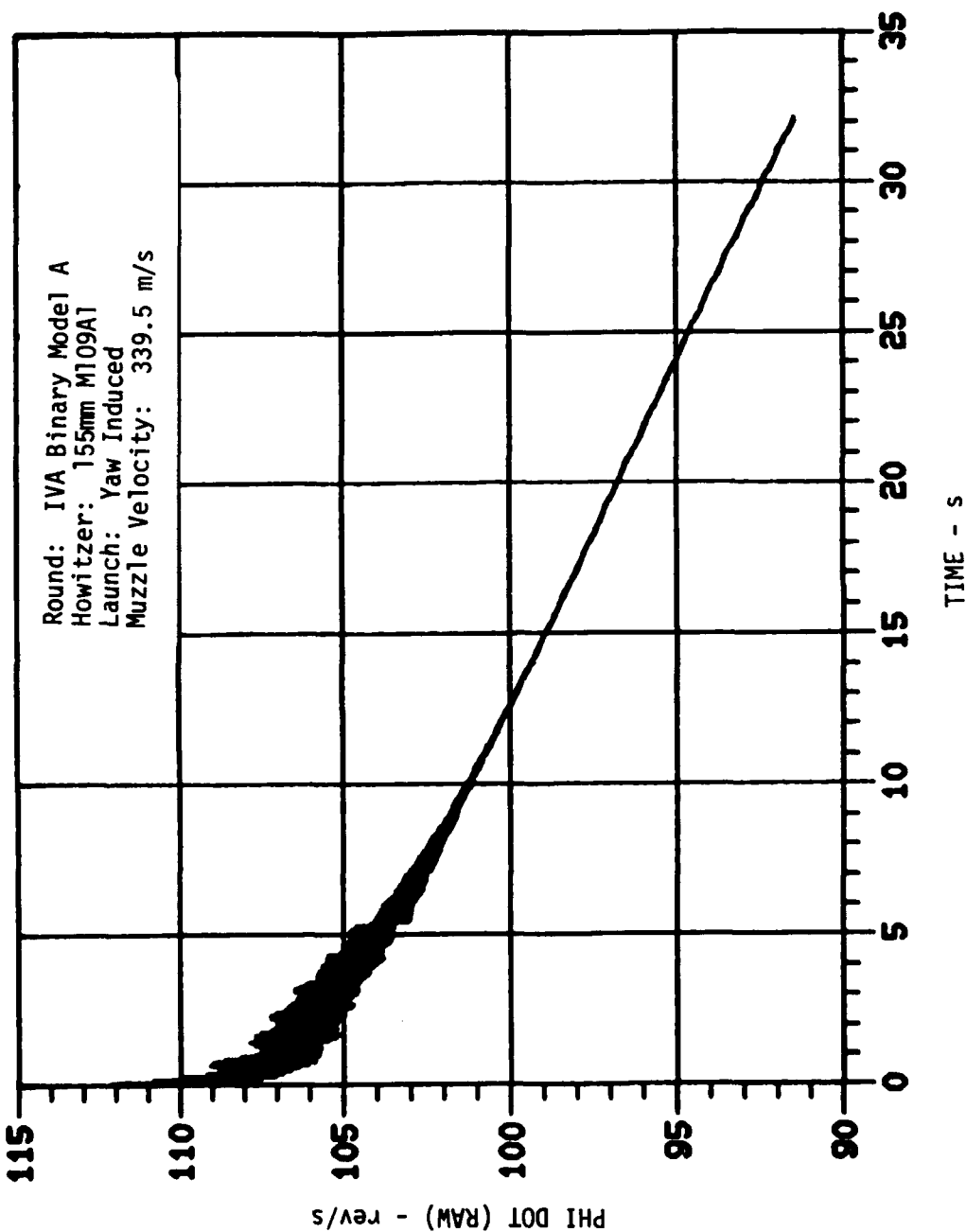


Figure 20. Phi Dot (Raw) versus Time (0-35 s) for Round 185A.

SITE I.D. CSL192B    BRL ROUND1714    FIRED    28AUG80

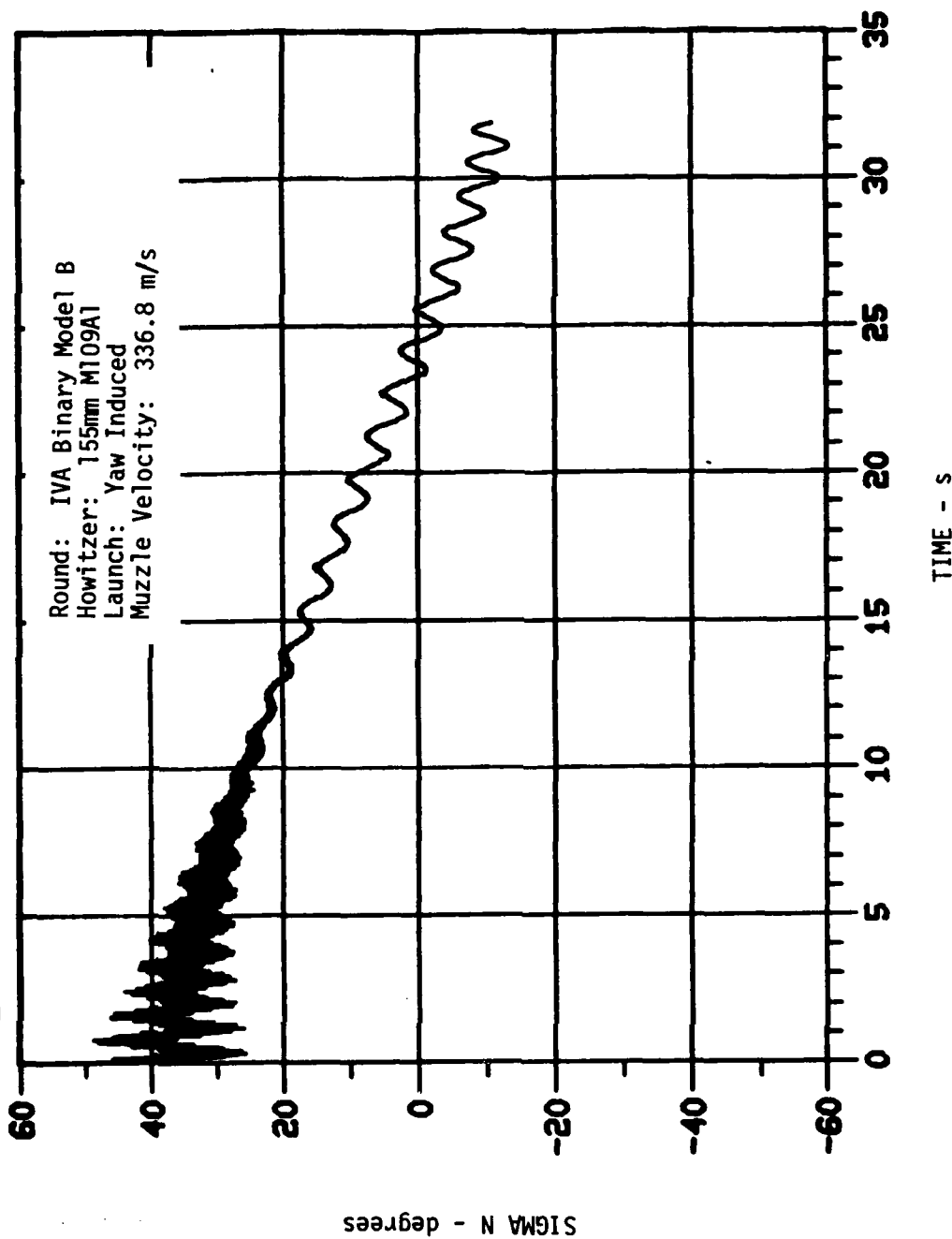


Figure 21. Sigma N versus Time (0-35 s) for Round 192B.

SITE I.D. CSL192B      BRL ROUND1714      FIRED      28AUG80

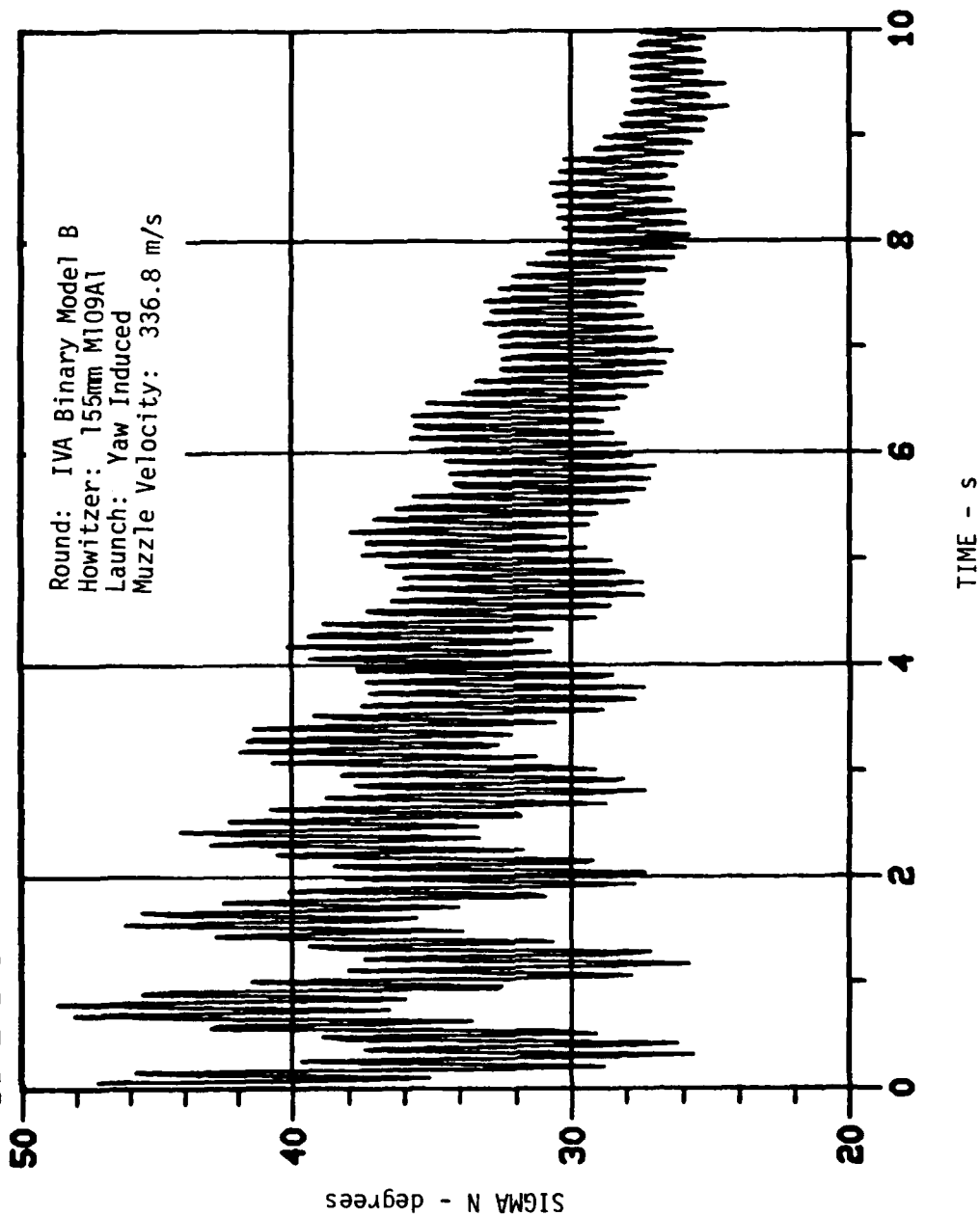


Figure 22. Sigma N versus Time (0-10 s) for Round 192B.

SITE I.D. CSL192B      BRL ROUND1714      FIRED      28AUG80

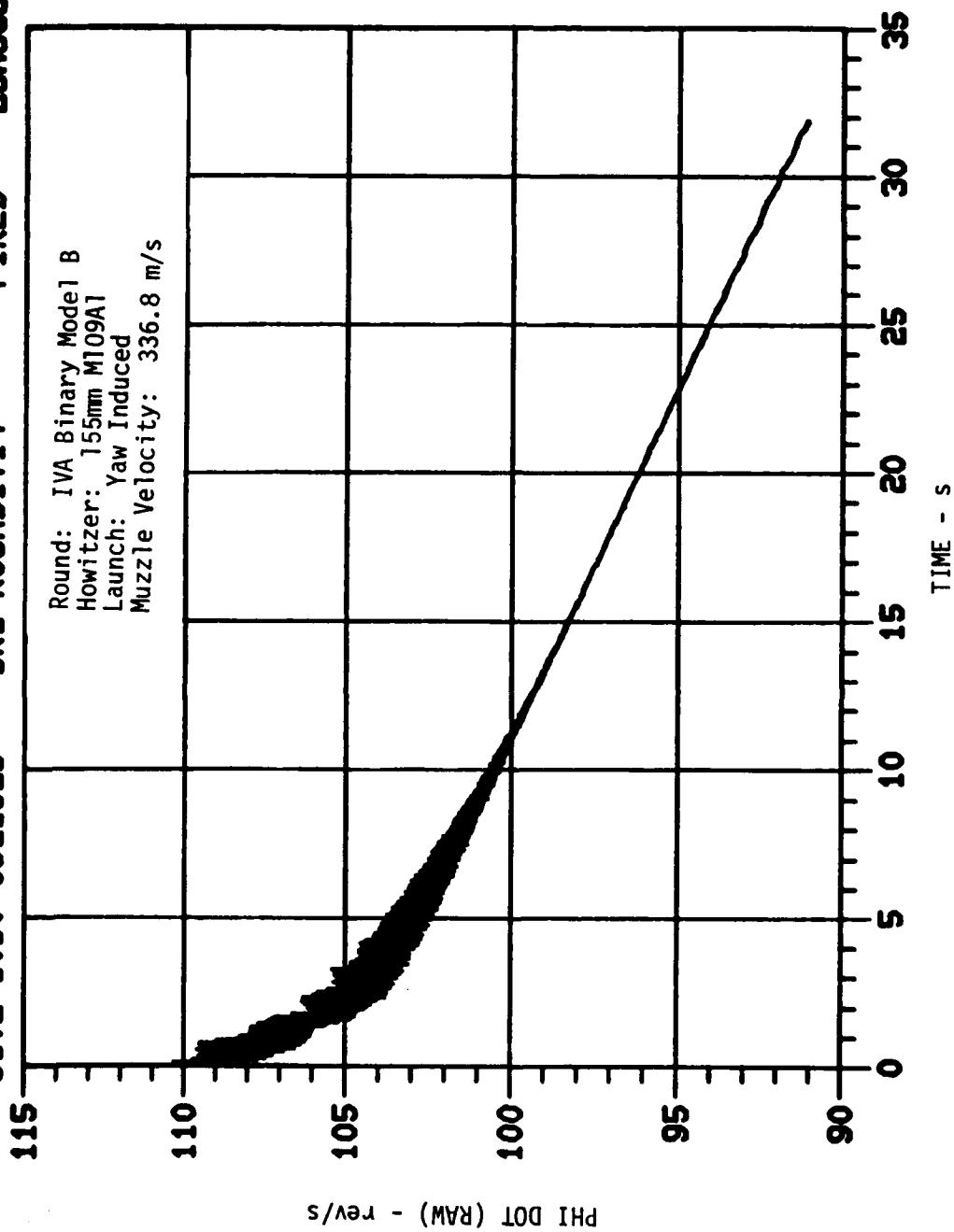


Figure 23. Phi Dot (Raw) versus Time (0-35 s) for Round 192B.

SITE I.D. CSL184A      BRL ROUND1715      FIRED      28AUG80

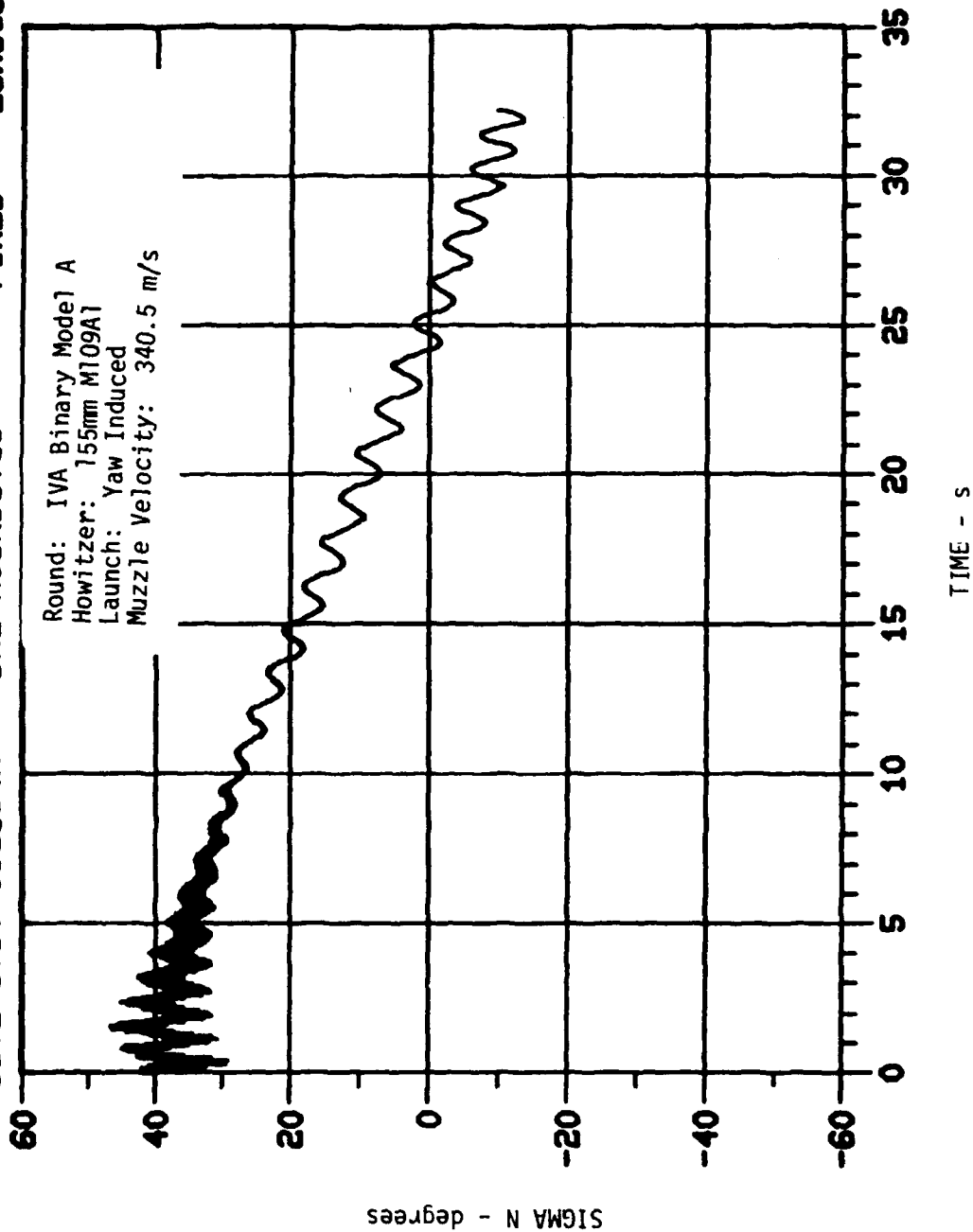


Figure 24. Sigma N versus Time (0-35 s) for Round 184A.



SITE I.D. CSL184A

BRL ROUND1715

FIRE

28AUG80

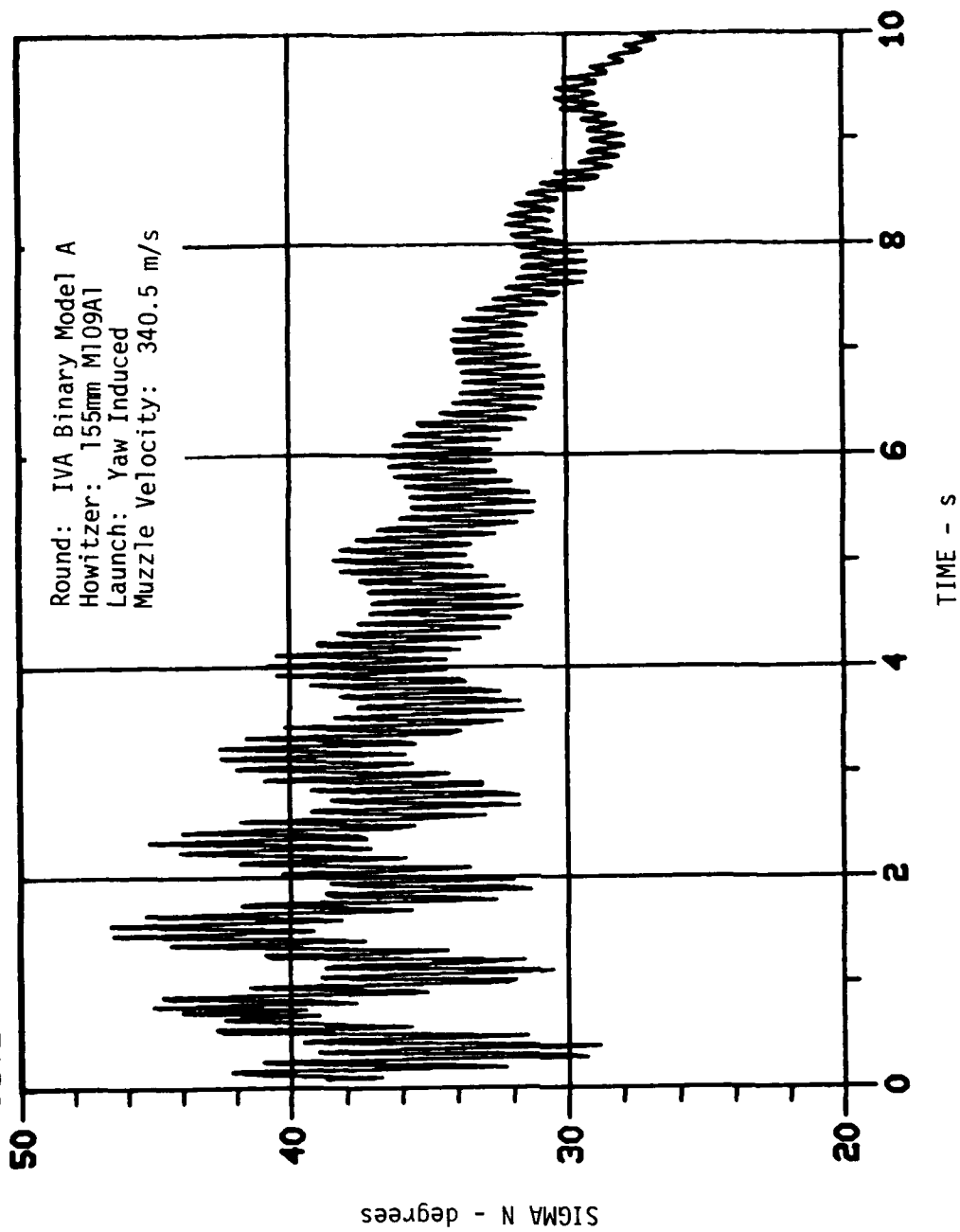


Figure 25. Sigma N versus Time (0-10 s) for Round 184A.

SITE I.D. CSL184A BRL ROUND1715 FIRED 28AUG80

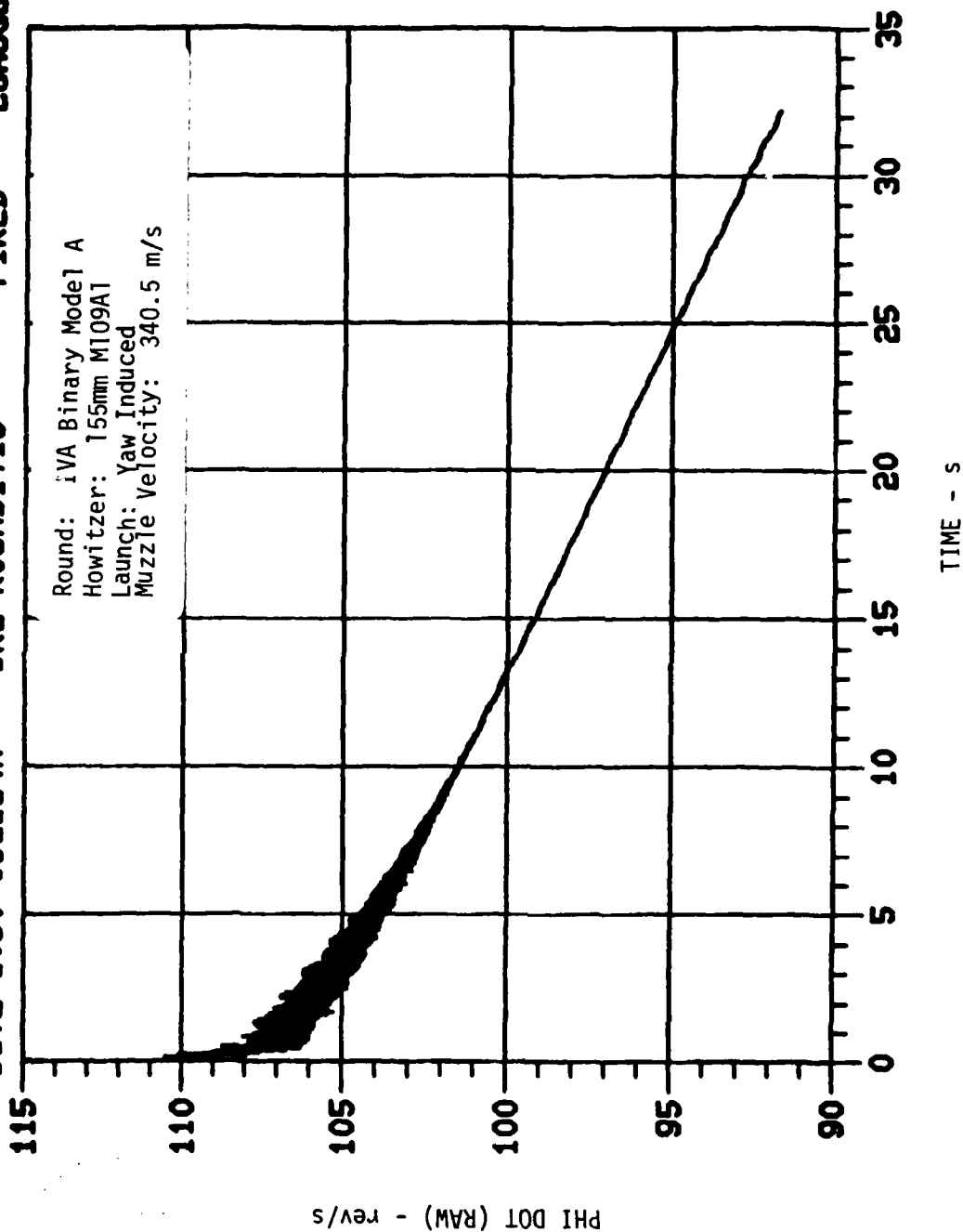


Figure 26. Phi Dot (Raw) versus Time (0-35 s) for Round 184A.

SITE I.D. CSL189B      BRL ROUND1624      FIRED      28AUG80

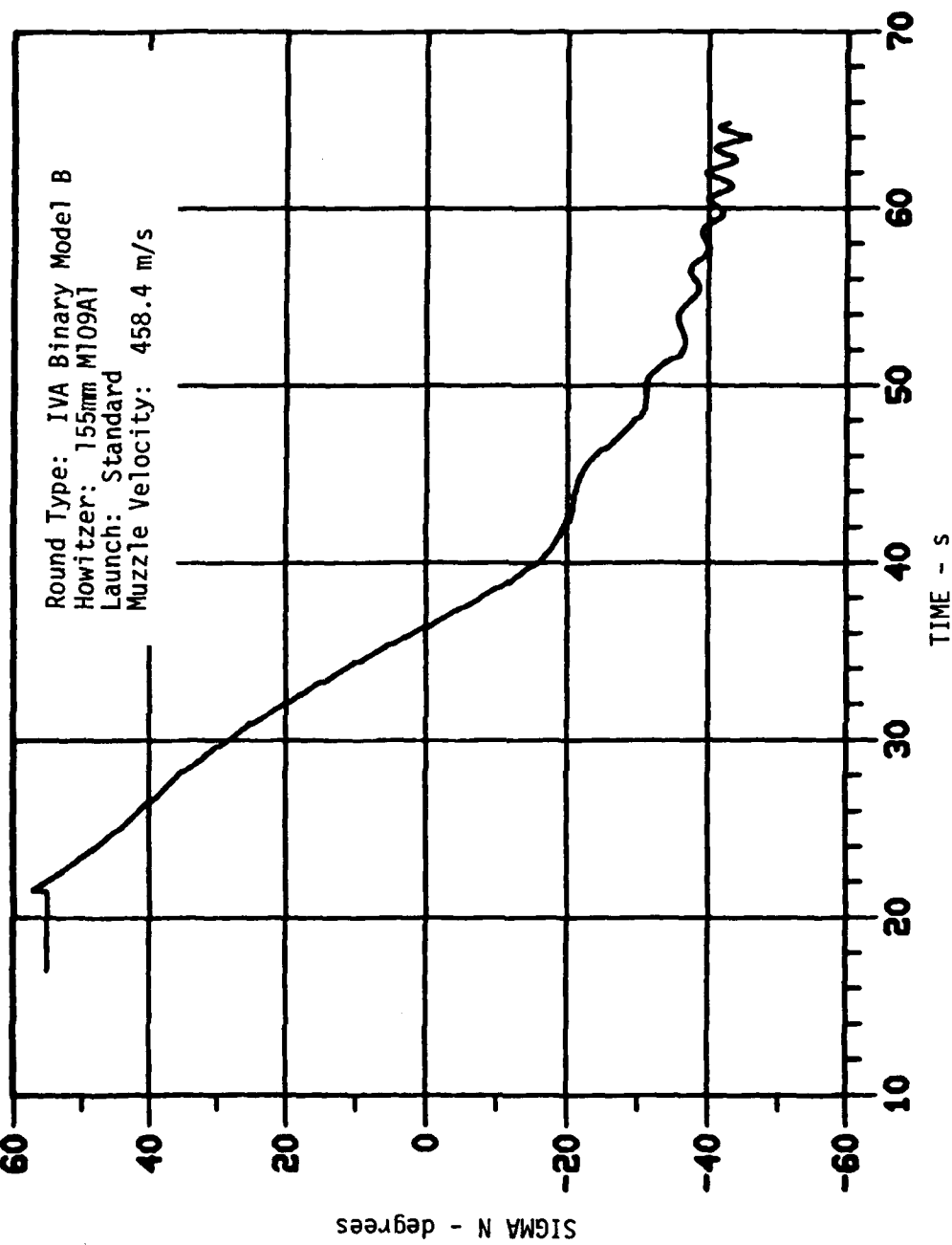


Figure 27. Sigma N versus Time (10-70 s) for Round 189B.

SITE I.D. CSL189B BRL ROUND1624 FIRED 28AUG80

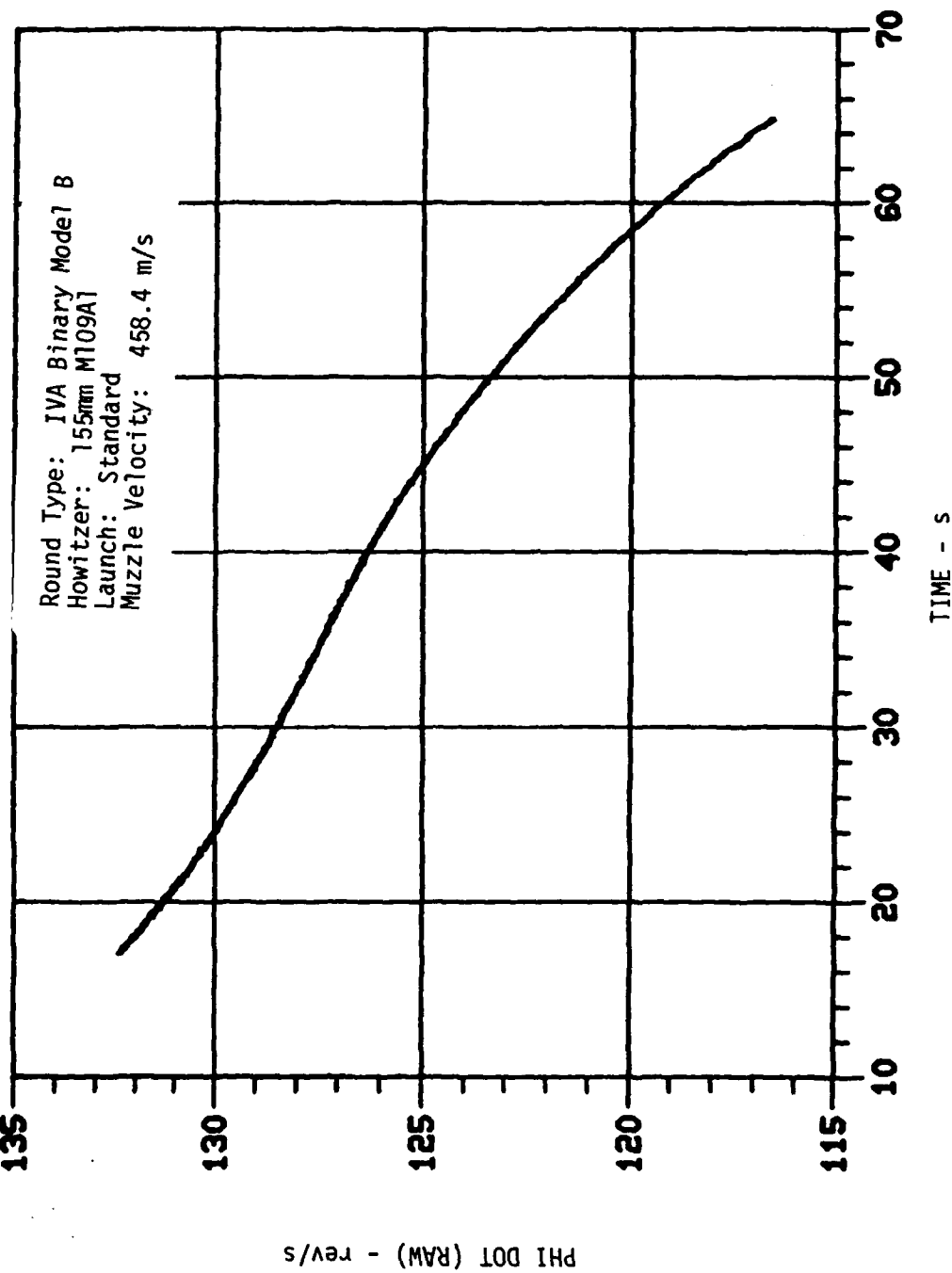


Figure 28. Phi Dot (Raw) versus Time (10-70 s) for Round 189B.

SITE I.D. CSL181A BRL ROUND1625 FIRED 28AUG80

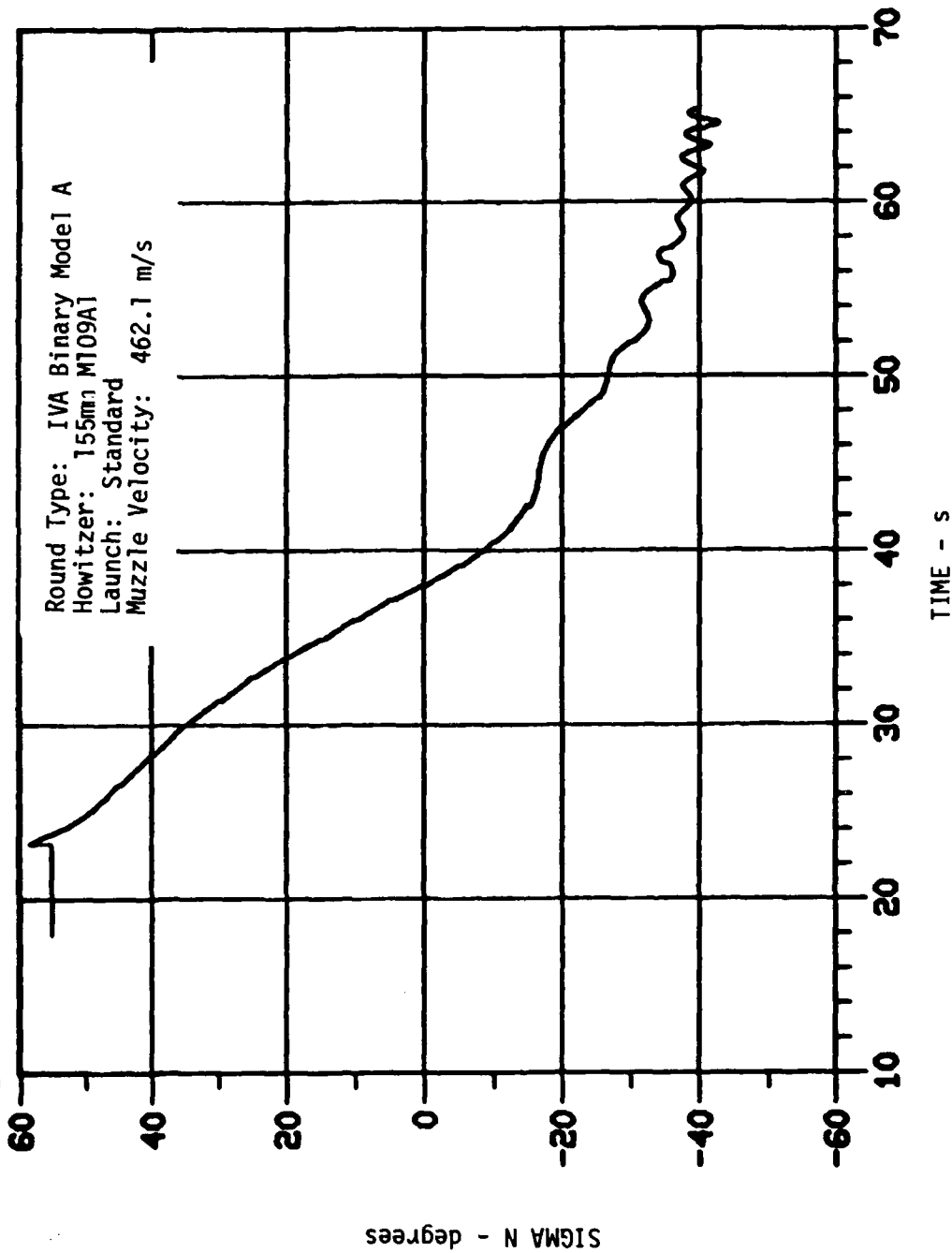


Figure 29. Sigma N versus Time (10-70 s) for Round 181A.

SITE I.D. CSL181A BRL ROUND1625 FIRED 28AUG80

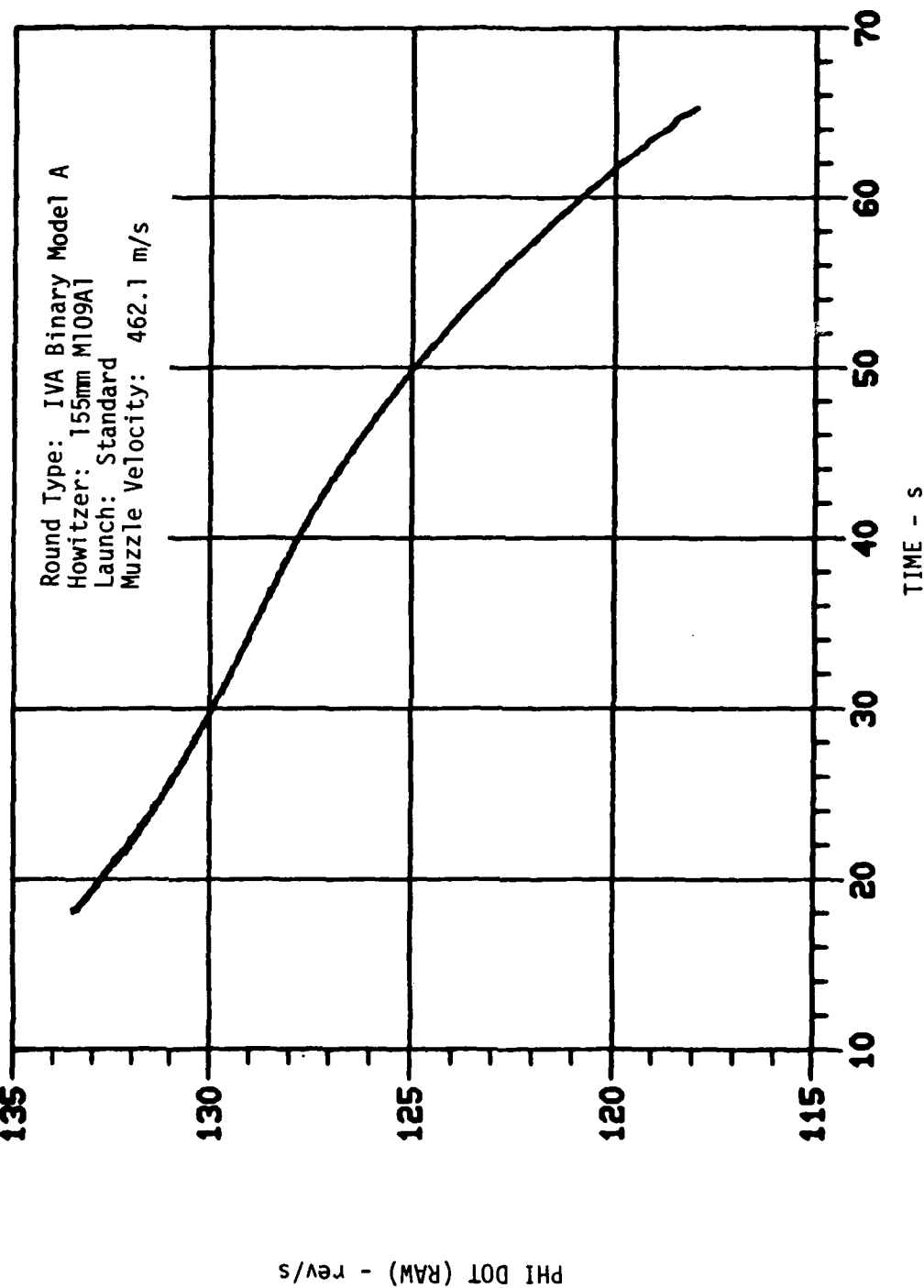


Figure 30. Phi Dot (Raw) versus Time (10-70 s) for Round 181A.

SITE I.D. CSL191B      BRL ROUND1716      FIRED      28AUG80

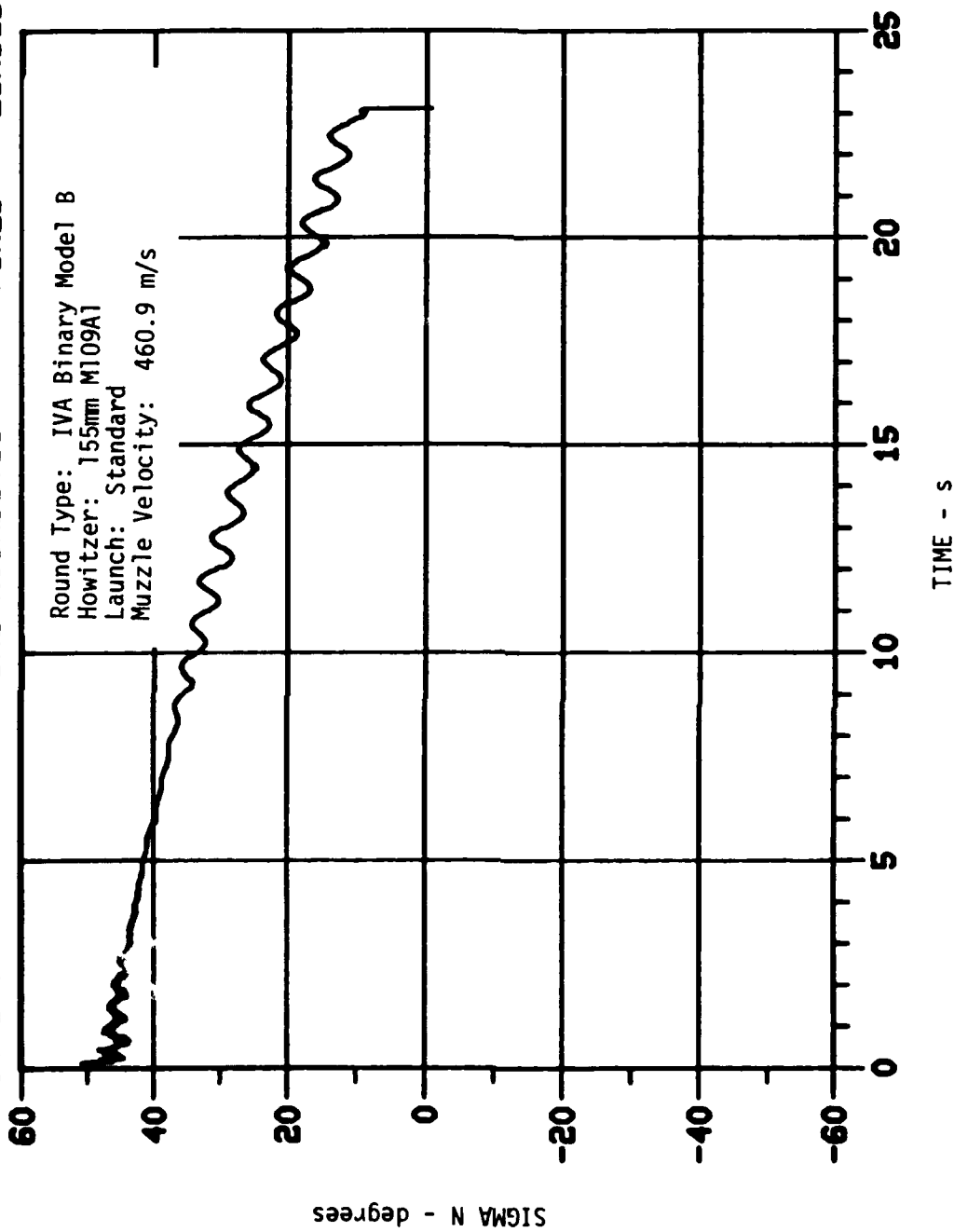


Figure 31. Sigma N versus Time (0-25 s) for Round 191B.

SITE I.D. CSL191B      BRL ROUND1716      FIRED      28AUG80

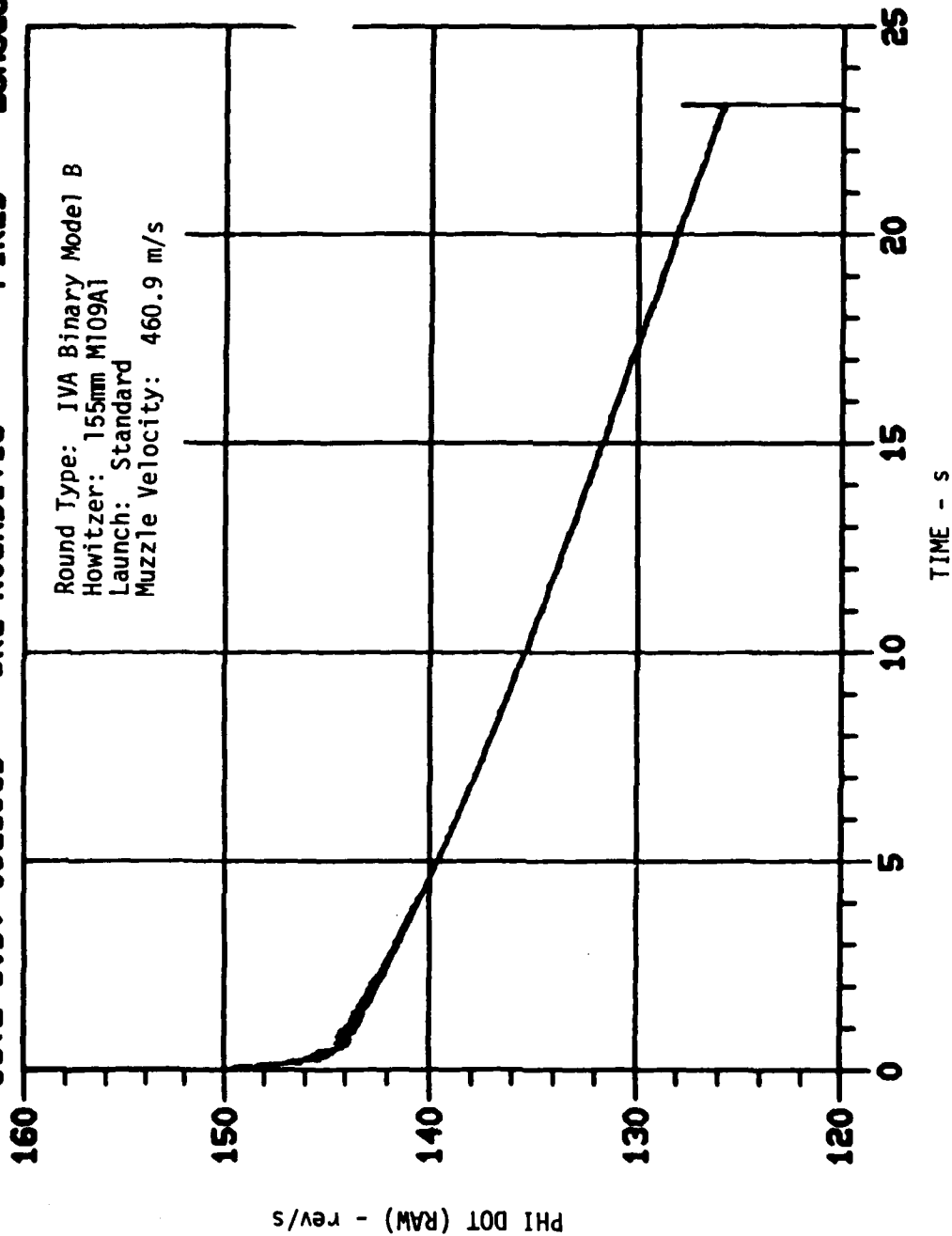


Figure 32. Phi Dot (Raw) versus Time (0-25 s) for Round 191B.



SITE I.D. CSL183A      BRL ROUND1697      FIRED      28AUG80

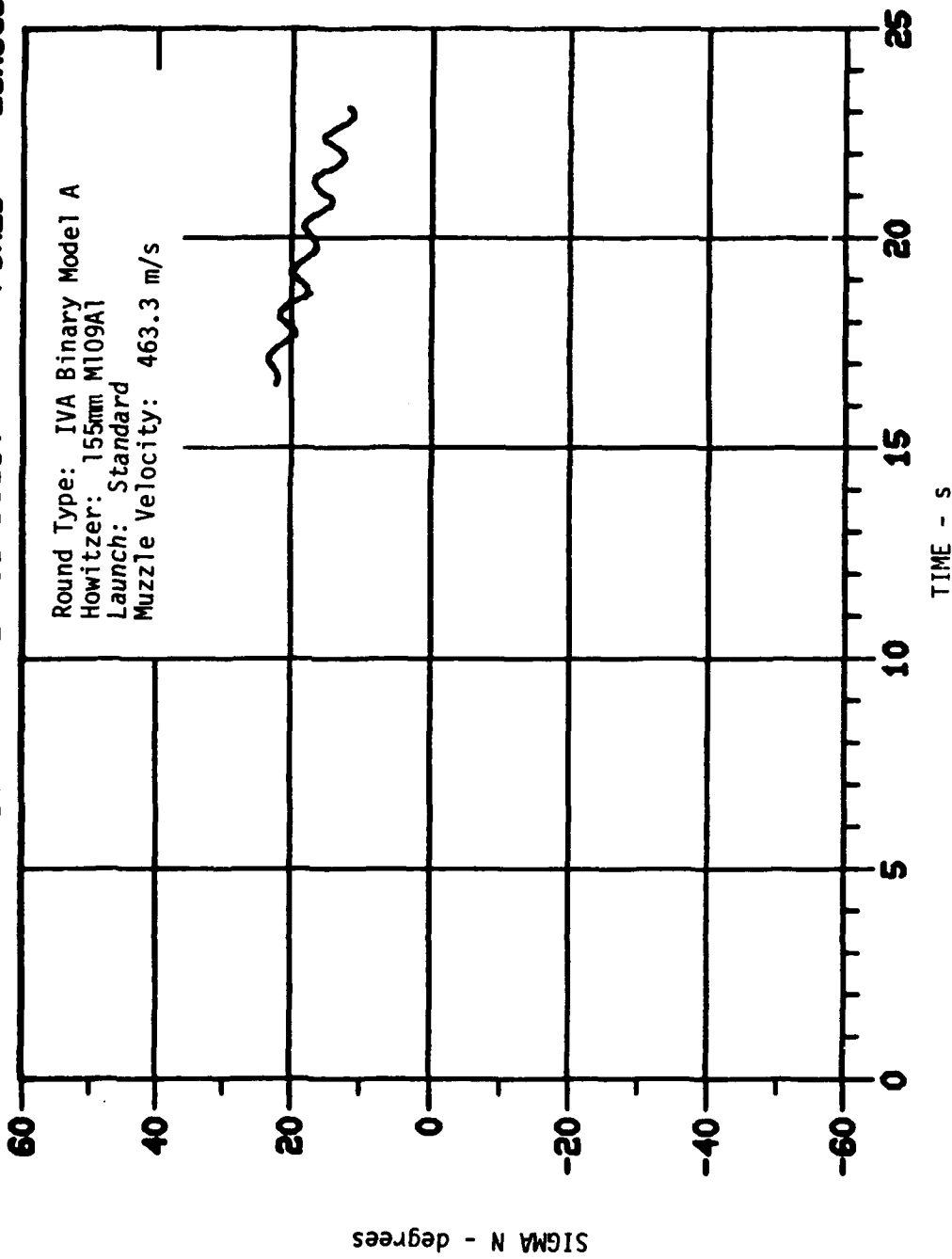


Figure 33. Sigma N versus Time (0-25 s) for Round 183A.

SITE I.D. CSL183A BRL ROUND1697 FIRED 28AUG80

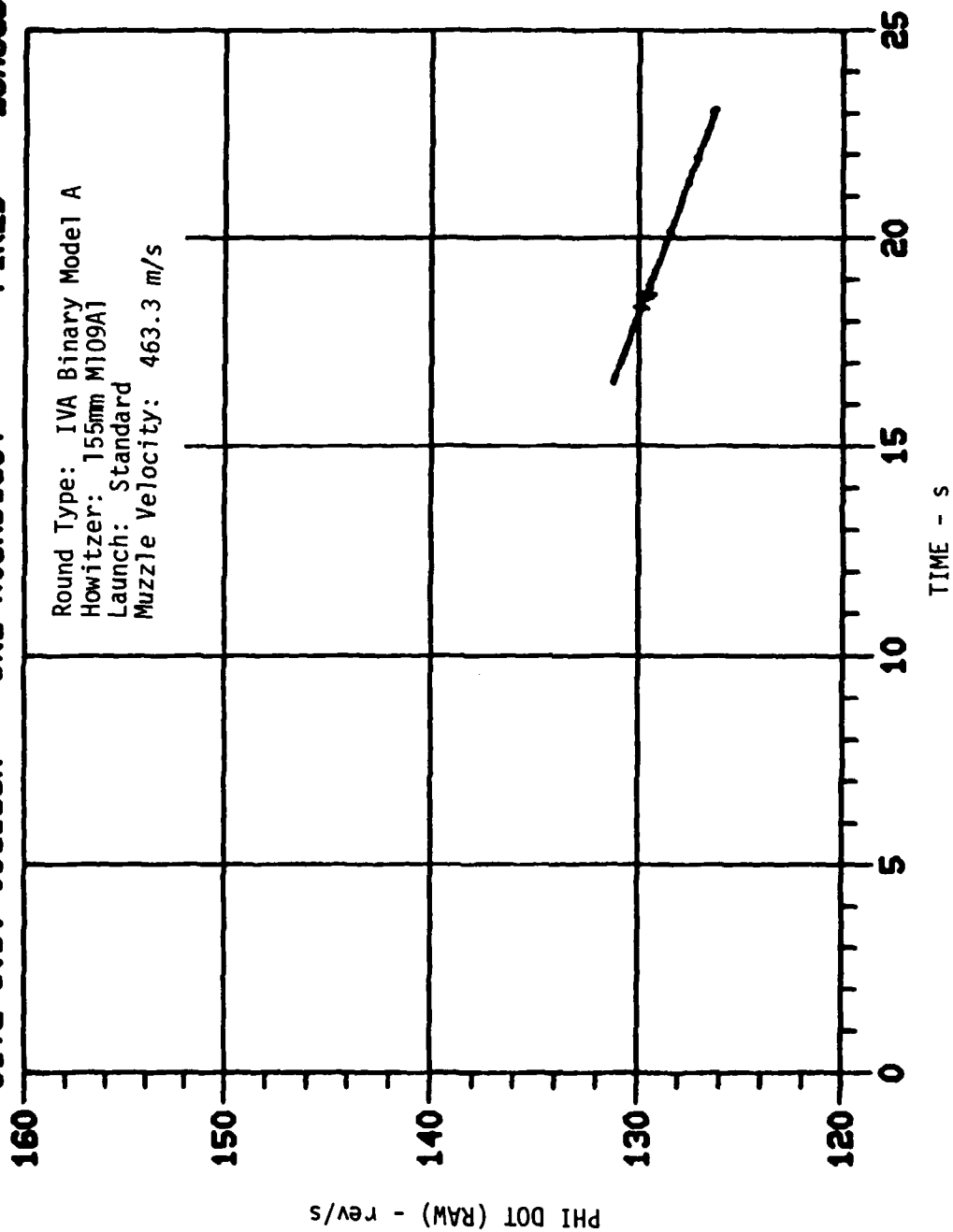


Figure 34. Phi Dot (Raw) versus Time (0-25 s) for Round 183A.

#### REFERENCES

1. K. Stewartson, "On the Stability of a Spinning Top Containing Liquid," J. Fluid Mech., Vol. 5, Part 4, September 1959, pp. 577-592.
2. E.H. Wedemeyer, "Viscous Corrections to Stewartson's Stability Criterion," BRL Report No. 1325, Aberdeen Proving Ground, Maryland, June 1966. AD 489687.
3. William P. D'Amico, Jr. and Michael D. Fuller, "Experimental Study of a Liquid-Filled Cylinder with Unequal Internal Diameters," BRL Memorandum Report in publication.
4. C.W. Kitchens, Jr. and N. Gerber, "Prediction of Spin-Decay of Liquid-Filled Projectiles," Ballistic Research Laboratories Report No. 1396, July 1977. AD A043275.
5. W.H. Mermagen and W.H. Clay, "The Design of a Second Generation Yawsonde," Ballistic Research Laboratories Memorandum Report No. 2368, April 1974. AD 780064.
6. C.H. Murphy, "Effect of Large High-Frequency Angular Motion of a Shell on the Analysis of Its Yawsonde Records," Ballistic Research Laboratory Memorandum Report No. 2581, February 1976. AD B009421L.

**BLANK PAGE**

# DISTRIBUTION LIST

<u>No. of Copies</u>	<u>Organization</u>	<u>No. of Copies</u>	<u>Organization</u>
12	Administrator Defense Technical Info Center ATTN: DTIC-DDA Cameron Station Alexandria, VA 22314	1	Director US Army Air Mobility Research and Development Laboratory Ames Research Center Moffett Field, CA 94035
1	Commander US Army Materiel Development and Readiness Command ATTN: DRCMD-ST 5001 Eisenhower Avenue Alexandria, VA 22333	1	Commander US Army Communications Research and Development Command ATTN: DRDCO-PPA-SA Fort Monmouth, NJ 07703
1	Commander US Army Armament Research and Development Command ATTN: DRDAR-TDC Dover, NJ 07801	1	Commander US Army Electronics Research and Development Command Technical Support Activity ATTN: DELSD-L Fort Monmouth, NJ 07703
5	Commander US Army Armament Research and Development Command ATTN: DRDAR-TSS (2 cys) DRDAR-LC, Dr. J. Frasier DRDAR-LCA-F, Mr. A. Loeb DRDAR-LCA-F, Mr. D. Mertz Dover, NJ 07801	1	Commander US Army Missile Command ATTN: DRSMI-R Redstone Arsenal, AL 35898
1	Commander US Army Armament Materiel Readiness Command ATTN: DRSAR-LEP-L, Tech Lib Rock Island, IL 61299	1	Commander US Army Missile Command ATTN: DRSMI-YDL Redstone Arsenal, AL 35898
1	Director US Army Armament Research and Development Command Benet Weapons Laboratory ATTN: DRDAR-LCB-TL Watervliet, NY 12189	1	Commander US Army Tank Automotive Research and Development Command ATTN: DRDTA-UL Warren, MI 48090
1	Commander US Army Aviation Research and Development Command ATTN: DRDAV-E 4300 Goodfellow Blvd. St. Louis, MO 63120	3	Project Manager Cannon Artillery Weapons Systems ATTN: DRCPM-CAWS US Army Armament Research and Development Command Dover, NJ 07801
		1	Director US Army TRADOC Systems Analysis Activity ATTN: ATAA-SL, Tech Lib White Sands Missile Range NM 88002

DISTRIBUTION LIST

<u>No. of Copies</u>	<u>Organization</u>
2	Sandia Laboratories ATTN: W.L. Oberkamp H. Vaughn Albuquerque, NM 87115
1	Aerospace Corporation ATTN: Walter F. Reddall El Segundo, CA 90245
2	Calspan Corporation ATTN: G. Homicz W. Rae P.O. Box 400 Buffalo, NY 14225

Aberdeen Proving Ground

Director, USAMSAA  
ATTN: DRXSY-D  
DRXSY-MP, H. Cohen

Commander, USATECOM  
ATTN: DRSTE-TO-F

PM SMOKE, Bldg. 324  
ATTN: DRCPM-SMK

Director, USACSL, EA  
Bldg. E3516  
ATTN: DRDAR-CLB-PA (1 cy)  
M. Miller (1 cy)

Director, USACSL, EA  
Bldg. E3330  
ATTN: W. Dee  
J. McKivriggan

### USER EVALUATION OF REPORT

Please take a few minutes to answer the questions below; tear out this sheet, fold as indicated, staple or tape closed, and place in the mail. Your comments will provide us with information for improving future reports.

1. BRL Report Number \_\_\_\_\_

2. Does this report satisfy a need? (Comment on purpose, related project, or other area of interest for which report will be used.)  
\_\_\_\_\_  
\_\_\_\_\_  
\_\_\_\_\_

3. How, specifically, is the report being used? (Information source, design data or procedure, management procedure, source of ideas, etc.) \_\_\_\_\_  
\_\_\_\_\_  
\_\_\_\_\_

4. Has the information in this report led to any quantitative savings as far as man-hours/contract dollars saved, operating costs avoided, efficiencies achieved, etc.? If so, please elaborate.  
\_\_\_\_\_  
\_\_\_\_\_  
\_\_\_\_\_

5. General Comments (Indicate what you think should be changed to make this report and future reports of this type more responsive to your needs, more usable, improve readability, etc.) \_\_\_\_\_  
\_\_\_\_\_  
\_\_\_\_\_  
\_\_\_\_\_

6. If you would like to be contacted by the personnel who prepared this report to raise specific questions or discuss the topic, please fill in the following information.

Name: \_\_\_\_\_

Telephone Number: \_\_\_\_\_

Organization Address: \_\_\_\_\_  
\_\_\_\_\_  
\_\_\_\_\_

----- FOLD HERE -----

Director  
US Army Ballistic Research Laboratory  
Aberdeen Proving Ground, MD 21005

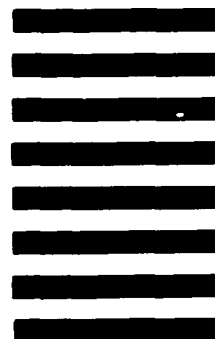


NO POSTAGE  
NECESSARY  
IF MAILED  
IN THE  
UNITED STATES

OFFICIAL BUSINESS  
PENALTY FOR PRIVATE USE, \$300

**BUSINESS REPLY MAIL**  
FIRST CLASS PERMIT NO 12062 WASHINGTON, DC  
POSTAGE WILL BE PAID BY DEPARTMENT OF THE ARMY

Director  
US Army Ballistic Research Laboratory  
ATTN: DRDAR-TSB  
Aberdeen Proving Ground, MD 21005



----- FOLD HERE -----